Event-related desynchronization during movement attempt and execution in severely paralyzed stroke patients: An artifact removal relevance analysis

Eduardo López-Larraz[a,*], Thiago C. Figueiredo[a], Ainhoa Insausti-Delgado[a,b,c], Ulf Ziemann[d], Niels Birbaumer[a,e], Ander Ramos-Murguialday[a,f]

[a] Institute of Medical Psychology and Behavioral Neurobiology, University of Tübingen, Germany
[b] International Max Planck Research School (IMPRS) for Cognitive and Systems Neuroscience, Tübingen, Germany
[c] IKERBASQUE, Basque Foundation for Science, Bilbao, Spain
[d] Department of Neurology & Stroke, and Hertie Institute for Clinical Brain Research, University of Tübingen, Germany
[e] Wyss Institute for Bio- and Neuroengineering, Genève, Switzerland
[f] Neural Engineering Laboratory, Health Department, TECNALIA, San Sebastián, Spain

A R T I C L E   I N F O

A B S T R A C T

The electroencephalogram (EEG) constitutes a relevant tool to study neural dynamics and to develop brain-machine interfaces (BMI) for rehabilitation of patients with paralysis due to stroke. However, the EEG is easily contaminated by artifacts of physiological origin, which can pollute the measured cortical activity and bias the interpretations of such data. This is especially relevant when recording EEG of stroke patients while they try to move their paretic limbs, since they generate more artifacts due to compensatory activity. In this paper, we study how physiological artifacts (i.e., eye movements, motion artifacts, muscle artifacts and compensatory movements with the other limb) can affect EEG activity of stroke patients. Data from 31 severely paralyzed stroke patients performing/attempting grasping movements with their healthy/paralyzed hand were analyzed offline. We estimated the cortical activation as the event-related desynchronization (ERD) of sensorimotor rhythms and used it to detect the movements with a pseudo-online simulated BMI. Automated state-of-the-art methods (linear regression to remove ocular contaminations and statistical thresholding to reject the other types of artifacts) were used to minimize the influence of artifacts. The effect of artifact reduction was quantified in terms of ERD and BMI performance. The results reveal a significant contamination affecting the EEG, being involuntary muscle activity the main source of artifacts. Artifact reduction helped extracting the oscillatory signatures of motor tasks, isolating relevant information from noise and revealing a more prominent ERD activity. Lower BMI performances were obtained when artifacts were eliminated from the training datasets. This suggests that artifacts produce an optimistic bias that improves theoretical accuracy but may result in a poor link between task-related oscillatory activity and BMI peripheral feedback. With a clinically relevant dataset of stroke patients, we evidence the need of appropriate methodologies to remove artifacts from EEG datasets to obtain accurate estimations of the motor brain activity.

1. Introduction

The electroencephalogram (EEG) allows studying the oscillatory activity associated to voluntary movement, which is a major area of interest within the fields of neurology and neurophysiology (Ramos-Murguialday and Birbaumer, 2015). The degree of motor cortex involvement during motor tasks has been largely studied and quantified by means of the event-related desynchronization of the alpha and beta rhythms (Pfurtscheller and Lopes da Silva, 1999). The existence of a tool to assess and quantify cortical involvement during motor tasks has

served, for instance, to characterize the pathological patterns of cortical activation of patients with motor disorders, such as stroke or spinal cord injury (Kaiser et al., 2012; López-Larraz et al., 2015; Park et al., 2016). It has also allowed to discover differences in oscillatory activity between stroke patients suffering subcortical and cortical lesions (Park et al., 2016; Ray et al., 2017; Stępień et al., 2011) and to study their cortical reorganization over time (Tangwiriyasakul et al., 2014b).

Measuring the cortical signatures of movement with EEG has also allowed the development of non-invasive systems that interpret those signals in real-time to create brain-machine interfaces (BMI) with

rehabilitative or assistive purpose (Chaudhary et al., 2016; Lebedev and Nicolelis, 2017; López-Larraz et al., 2018b). Different devices, including robotics and prosthetics, have been controlled by patients using brain activity only, to facilitate the movement of their paralyzed arms and legs (Hortal et al., 2015; Ibáñez et al., 2017; López-Larraz et al., 2016). The use of these systems to provide a contingent proprioceptive feedback has been demonstrated to promote neural plasticity and motor learning in healthy individuals and patients (Mrachacz-Kersting et al., 2012; Mrachacz-Kersting et al., 2016; Ramos-Murguialday et al., 2012). Further, BMI-based rehabilitation interventions have proven their success in promoting clinical improvements after stroke and spinal cord injury (Ang et al., 2015; Biasiucci et al., 2018; Donati et al., 2016; Ono et al., 2014; Pichiorri et al., 2015; Ramos-Murguialday et al., 2013; Trincado-Alonso et al., 2018). The key point of these interventions is to establish a link that associates the neural activity related to voluntary movement and the peripheral feedback to facilitate plasticity by Hebbian mechanisms (Jackson and Zimmermann, 2012).

The main limitation of EEG recordings, either for neurophysiological assessment or for BMI development, is its low signal to noise ratio and easiness to get contaminated. Generally, several tens of repetitions (i.e., trials) of the same task have to be recorded and averaged to derive an accurate estimate of the brain process of interest, or to calibrate the classification algorithm for the BMI (Graimann and Pfurtscheller, 2006). Interferences of electrical or physiological origin (i.e., artifacts) contaminate the EEG signals, potentially biasing the information and interpretations that can be extracted from these data. Electrical artifacts can be avoided by following good practices, such as recording the EEG data in an electrically shielded room, using battery-powered devices, and minimizing electrode impedances (Hammond and Gunkelman, 2001; Nunez and Srinivasan, 2006). When these artifacts are produced by the sources of stimulation used by a BMI (e.g., closed-loop electric or magnetic stimulation), they can induce a bias in the estimation of EEG power. Different methods have been proposed to avoid this phenomenon, such as ignoring or interpolating the contaminated portions of signal (Hoffmann et al., 2011; Walter et al., 2012) or using median filtering to minimize the peaks (Insausti-Delgado et al., 2017). Physiological artifacts can be largely reduced by instructing the subjects on how to avoid them; however, sometimes their occurrence is unavoidable. The most common physiological contaminations of EEG recordings are caused by: (1) electrooculographic (EOG) activity, which generates electrical currents due to eyelid movements and movements of the retinal dipoles (Schlögl et al., 2007); (2) motion artifacts, with low-frequency, high-amplitude oscillations as a result of (involuntary) head or body movements during the execution or attempt of other movements (Castermans et al., 2014); and (3) muscular artifacts, which produce power increases in high-frequencies of the EEG due to the overlap with the spectral bandwidth of muscle activity (Muthukumaraswamy, 2013).

Dozens of methods are currently available to try to minimize the influence of each type of artifact in EEG recordings (Croft and Barry, 2000; Muthukumaraswamy, 2013; Urigüen and Garcia-Zapirain, 2015). However, there are four important problems missing in the literature that can be of crucial importance, especially when working with EEG of patients with motor paralysis (e.g., due to stroke). Firstly, most of the works study the effects of "cleaning" the artifacts on the resulting signals only; not quantifying, for instance, the differences in the estimation of cortical activation or in BMI performance (Urigüen and Garcia-Zapirain, 2015). Secondly, they generally measure the influence of artifacts in healthy individuals, although there might be differences in how these contaminations affect data of healthy vs. paralyzed subjects (López-Larraz et al., 2017a), since patients generate more compensatory activity during attempts of movement. Thirdly, assuming that artifacts are just additive noise that lowers the signal-to-noise ratio can be problematic; if the artifacts are somehow correlated with the studied task (e.g., muscular contamination of the EEG due to excessive contraction during movement attempt), they can be learned by the BMI

classifier, leading to an optimistic bias in its performance (Castermans et al., 2014). Fourthly, in addition to the EEG artifacts, compensatory movements of limbs not related to the task are commonly ignored, although they can also bias the measurement of cortical activity (Ramos-Murguialday et al., 2010).

Given the growing interest in the use of EEG and EEG-based BMIs to improve the assessment and motor rehabilitation of patients with paralysis due to stroke, the appropriate cleaning of these signals might be of paramount importance to obtain accurate estimations of brain activation. This work aims at measuring the influence of physiological artifacts in EEG recordings of stroke patients on the quantification of cortical activity and for the use of rehabilitative BMI systems. We expect that more restrictive artifact rejection procedures will lead to a more accurate estimation of the cortical activity during a motor task, which should also result in a better link between the brain and the paralyzed muscles in a BMI therapy. We analyzed a clinically relevant dataset of 31 severely paralyzed stroke patients to study the effects of rejecting EEG and EMG artifacts from an electrophysiological and from a neurotechnological point of view.

2. Materials and methods

2.1. Patients

Thirty-one chronic stroke patients (19 male, mean age 54.0 ± 11.7 years, range 29–73, time since stroke 60.3 ± 58.2 months, range 10–232) were recruited for this study. Inclusion criteria were: (1) hand paralysis with no finger extension; (2) minimum time since stroke 10 months; (3) age between 18 and 80 years; (4) no psychiatric or neurological condition other than stroke; (5) no cerebellar lesion or bilateral motor deficit; (6) no pregnancy; (7) no epilepsy or medication for epilepsy during the last 6 months; (8) eligibility to undergo magnetic resonance imaging (MRI); and (9) ability to understand and follow instructions. Demographic and clinical data of the patients can be found in Table 1. Further details about the lesion location and the brain areas affected by the stroke in each patient can be found in Supplementary Table 1 and Supplementary Fig. 1. The experiments were conducted at the University of Tübingen, Germany. The experimental procedure was approved by the ethics committee of the Faculty of Medicine of the University of Tübingen, and all the patients provided written informed consent.

2.2. Experimental design and procedure

The patients were asked to perform an assessment task in which they had to move their healthy hand, or to attempt to move their paralyzed hand, while their electroencephalographic (EEG) and electromyographic (EMG) activity was recorded. Each patient performed between 4 and 6 blocks, each of which contained, in a random order, 17 trials of movement execution (healthy hand) and 17 trials of movement attempt (completely paralyzed hand). The number of blocks recorded depended on the tiredness of the patients, as in some cases they requested to stop the measurements before finishing the 6 expected blocks.[1] Audiovisual cues guided the patients regarding the phases of a trial: rest (random duration between 4 and 5 s), movement execution/attempt (4 s), and an inter-trial interval that was included every three trials (random duration between 8 and 9 s). The patients were asked to perform (or try to perform) openings and closings with their healthy (or paretic) hand at a comfortable personal pace during the 4 s of the movement execution/attempt interval (generally, it took them around 1.5 s to perform a complete open-close cycle). Before starting the first

---

[1] In a post-hoc analysis, we verified that there were no significant differences due to the unequal amount of trials for each patient in terms of estimated cortical activity and BMI accuracy.

Table 1
Patients demographic data. Lesion side indicates the damaged hemisphere. Lesion type indicates if the stroke affected subcortical areas only (S) or cortical and subcortical areas (C + S). cFMA stands for combined Fugl-Meyer assessment, which comprises hand and arm motor scores combined, excluding co-ordination, speed and reflexes (range 0–54 points, with 54 points indicating normal hand/arm function).

ID	Gender	Age (yr)	Time since stroke (mo)	Lesion side	Lesion type	cFMA
1	M	60	14	R	C + S	13
2	F	52	156	L	C + S	5.5
3	F	66	23	L	C + S	16.5
4	F	54	10	L	C + S	8
5	M	58	28	R	C + S	8.5
6	M	62	10	R	C + S	1
7	F	73	23	R	C + S	1
8	M	60	130	L	S	9.5
9	F	36	16	L	C + S	11
10	M	57	122	R	S	17
11	M	47	80	R	S	12
12	M	51	16	L	C + S	3.5
13	M	69	89	R	C + S	26
14	F	35	28	R	C + S	11
15	F	72	44	L	S	2
16	F	55	17	R	S	0.5
17	M	66	48	R	C + S	7.5
18	M	69	72	L	S	5.5
19	F	55	45	L	S	16.5
20	F	53	30	L	S	5
21	F	35	60	R	S	25.5
22	M	58	28	R	C + S	8.5
23	M	29	25	R	C + S	15
24	M	47	232	R	C + S	13.5
25	M	50	215	L	S	33.5
26	M	48	45	R	S	7.5
27	F	53	20	L	S	17.5
28	M	40	53	R	C + S	3.5
29	M	70	23	L	C + S	8
30	M	40	46	L	S	30.5
31	M	54	121	R	C + S	16

block, they were instructed to minimize compensatory movements and any other source of contamination for the EEG activity during the rest and movement intervals.

2.3. Data recording and preprocessing

EEG activity was recorded using a commercial Acticap system (BrainProducts GmbH, Germany), with 16 electrodes placed on Fp1, Fp2, F3, Fz, F4, T7, C3, Cz, C4, T8, CP3, CP4, P3, Pz, P4, and Oz (according to the international 10/20 system). The ground and reference electrodes were placed on AFz and FCz, respectively. Vertical and horizontal electrooculography (EOG) was also recorded to capture eye movements. Electromyographic activity was recorded using bipolar Ag/AgCl electrodes (Myotronics-Noromed, USA) from four muscle groups of each arm: *extensor carpi ulnaris*, *extensor digitorum*, external head of the *biceps* and external head of the *triceps*. All signals were synchronously recorded at 500 Hz.

The EEG data were filtered between 0.1 and 48 Hz with a 4-th order causal Butterworth filter. The signals were trimmed down to 7-s trials, from −3 to +4 s with respect to the movement cue. Although the shortest duration of the rest intervals was 4 s, we decided to consider only the last 3 s to ensure that the patients were in resting state.

2.4. Artifact rejection procedures

The artifact rejection procedures were designed to identify and minimize the influence of four types of contaminations that can frequently occur when measuring EEG activity during movement executions or attempts: electrooculographic contaminations, motion artifacts,

muscle artifacts, and compensatory movements with other limbs. For that, we relied on the recorded EEG and EMG activities. Three different methods were proposed and compared between them and with no artifact rejection: (1) artifact rejection based on EMG activity only; (2) artifact rejection based on EEG activity only; (3) artifact rejection based on EMG and EEG. The EMG activity was used to identify undesired compensatory movements with the arm that the patients should keep relaxed. The EEG (and EOG) activity was used to detect electrooculographic contaminations, motion artifacts and muscle artifacts. These artifact rejection procedures were applied to the available set of trials of each patient: i.e., to all the trials of the patient when applied for quantifying the brain activation, and only to the trials used to train the BMI for detecting the movement execution/attempts (see Sections 2.5 and 2.6). The processing of artifacts was done on a single trial basis: i.e., each trial was processed and marked as clean or as contaminated, and when marked as contaminated it was discarded.

2.4.1. Artifact rejection based on EMG

The EMG activity was used to identify trials with undesired movements of the arms, which might generate cortical activity that masks the activity of interest (more than physiologic artifacts, these trials correspond to an incorrect performance of the requested task). This method is referred to as "EMG rejection". We defined as artifacts those trials that had: (1) muscular activations in any of the recorded muscles during the rest intervals; or (2) muscular activations in the muscles of the opposite arm to the one requested to move (e.g., compensatory movements with the healthy arm during the attempt of movement of the paretic hand).

The processing of the EMG signals was as follows. First, the EMG of each trial was high-pass filtered at 20 Hz with a 4th-order non-causal Butterworth filter. The waveform length (WL) was computed in 200 ms windows with a sliding step of 20 ms, as in (Ramos-Murguialday et al., 2010). The WL values of the rest interval (i.e., [−3, 0] s) of each trial were averaged, and the mean and standard deviation (SD) between trials were used to compute the rejection threshold: i.e., 3 SD above the mean. Those rest intervals presenting WL values higher than this threshold for a duration longer than 200 ms were considered artifacts and discarded. Subsequently, the mean and SD of the non-rejected trials were computed and used to re-calculate the rejection threshold (i.e., 3 SD above the new mean). Those trials in which this threshold was exceeded for > 200 ms were considered as artifacts if: (1) the activation occurred in any muscle during the rest interval (i.e., [−3, 0] s); or (2) the activation occurred in any of the muscles of the opposite arm to the moving one during the movement interval (i.e., [0, 4] s).

2.4.2. Artifact rejection based on EEG

Our method to reject artifacts relying on EEG activity was first presented in (López-Larraz et al., 2017a) and aims at eliminating the three main (physiological) sources of contamination: eye movements, motion artifacts, and muscle artifacts. This procedure is referred to as "EEG rejection" and involves one step of EOG removal (or correction) and two steps of rejection of trials with artifacts. The influence of eye movements on the EEG was corrected by using linear regression on the EOG data; a method that constitutes one of the state-of-the-art procedures to remove undesired ocular activity while keeping the relevant brain information (Kobler et al., 2017; Urigüen and Garcia-Zapirain, 2015). On the other hand, motion artifacts and muscle artifacts are more difficult to "clean" (i.e., to filter the contamination while maintaining the amount of trials), and there is disagreement in the literature about the effectiveness of techniques to correct these contaminations (Kline et al., 2015; Muthukumaraswamy, 2013; Urigüen and Garcia-Zapirain, 2015). Therefore, we implemented a statistical procedure to identify trials containing artifacts and to completely discard them. Note that not all the EEG channels were considered for the identification of artifacts, but only the ones that were involved in the corresponding analysis (see Sections 2.5 and 2.6). For instance, when detecting the

attempts of movement using the contralateral EEG electrodes, only the contralateral electrodes and their neighbors (used to re-reference by Laplacian derivations) were considered.

2.4.2.1. Removal of ocular artifacts.
The horizontal and vertical components of eye movements were removed from the EEG by using linear regression between the EEG and EOG activities, as proposed in (Schlögl et al., 2007). This method assumes that the measured EEG signals are a linear combination between the brain activity and the contamination due to eye movements:

$$X_{c,t} = EEG_{c,t} + b_{c,d} \times EOG_{d,t} \tag{1}$$

where $X_{c,t}$ represents the recorded EEG signals, measured in c electrodes during t time points; $EEG_{c,t}$ is the actual brain activity; $EOG_{d,t}$ are the derivations of electrooculographic activity (in our case $d = 2$, with horizontal and vertical EOG derivations); and $b_{c,d}$ are the coefficients that represent the weights of the EOG contamination of each EEG channel. The coefficients b are estimated as the product of the auto-covariance matrix of the EOG derivations and the cross-covariance between the EEG and EOG. After that, the brain activity clean of ocular contaminations is calculated by subtracting the weighted contaminations from the measured signals:

$$EEG = X - b \times EOG \tag{2}$$

It is possible to estimate the coefficients b from a given segment of data and clean such data (i.e., offline analysis), or to apply these coefficients to new, unseen data (i.e., for online filtering). Therefore, this method corrects the artifacts (i.e., removes the contamination) but preserves the amount of trials.

2.4.2.2. Rejection of motion artifacts and muscle artifacts.
The rejection of these two types of artifacts was done using a similar statistical method to the one used with the EMG activity (see 2.4.1). Motion artifacts are generally characterized by low frequency oscillations, while muscular artifacts can be observed in the EEG in high frequencies. To capture those artifacts, we computed the spectral power in delta ([1–4] Hz) and gamma ([30–48] Hz) for the rest and for the movement intervals of each trial (i.e., one value per frequency band and interval for each trial). The mean and SD of delta and gamma power during the rest intervals were used to define the first rejection threshold (3 SD above the mean of each band). All those trials exceeding this threshold in the rest interval were discarded. We recalculated the rejection threshold for each band using the rest interval of the non-rejected trials only, and also discarded all the trials that exceeded this new threshold in any of the bands in the rest or in the movement intervals.

2.4.3. Artifact rejection based on EMG and EEG
The last method was the most restrictive and combined the use of both EMG and EEG activity to identify trials with undesired movements, eye movements, motion artifacts or muscle artifacts. This method is referred to as "EMG + EEG rejection". Firstly, trials with undesired movements (i.e., malperformance of the task) were rejected by using the method described in Subsection 2.4.1. Secondly, the remaining trials were processed with the methods detailed in Subsection 2.4.2 to eliminate eye movements, motion artifacts, and muscle artifacts.[2]

---

[2] The order of this sequential process (EMG rejection followed by EEG rejection) was chosen to first eliminate the trials in which the task was performed incorrectly, and then to compute the statistical parameters for rejection of motion and muscle artifacts from the trials in which the task was performed correctly. In a post-hoc analysis, we compared the effect of reversing this process (EEG rejection followed by EMG rejection), obtaining no significant differences between both approaches.

2.5. Quantification of cortical activity

The degree of cortical activation during motor execution and motor attempt was quantified by computing the event-related synchronization/desynchronization (ERS/ERD) of the central alpha ([7–13] Hz) and central beta ([14–30] Hz) rhythms (Pfurtscheller and Lopes da Silva, 1999). Fig. 1-A displays the flowchart with the processing steps to compute the ERS/ERD. First, the artifact rejection methods were applied to the trials of each patient separately. Afterwards, the data of all the patients were pooled together to study the average activation for each condition.

The EEG signals were re-referenced using small Laplacian derivations to reduce the effect of volume conduction (Hjorth, 1975). Time-frequency maps representing the cortical activity were computed using Morlet Wavelets (Tallon-Baudry et al., 1997) in the frequency range [1–50] Hz, with a frequency resolution of 0.25 Hz. In these time-frequency maps, the percentage of relative power decrease with respect to a resting-state baseline ([−2.5, −1] s) was calculated to obtain the ERS/ERD patterns, and their statistical significance was estimated using a bootstrap resampling method (Graimann and Pfurtscheller, 2006).

For each patient and artifact rejection method, the mean ERS/ERD percentage in alpha and beta frequencies was computed from the time-frequency maps of the channels C3 and C4 (i.e., as descriptors of the left- and right-hemispheric sensorimotor cortex, respectively). For that, the ERS/ERD values in the frequency ranges [7–13] Hz (alpha) and [14–30] Hz (beta) were averaged in the time interval [0, 4] s. Higher magnitude of ERD activity (i.e., more negative values) is related to higher cortical activation during motor tasks (Pfurtscheller and Lopes da Silva, 1999), while muscular contaminations tend to generate ERS activity. Therefore, we would expect that cleaner EEG datasets display ERD values of higher magnitude.

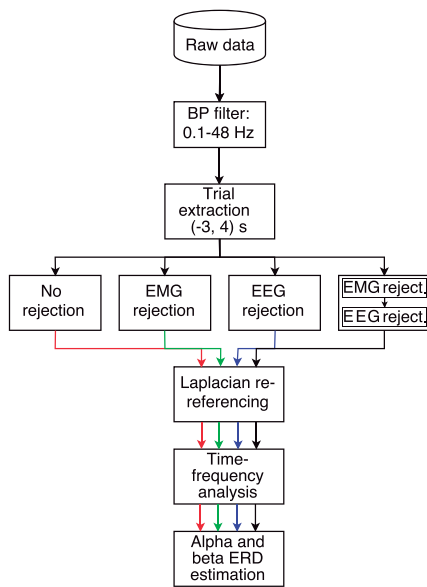### 2.6. Movement execution/attempt detection

2.6.1. Design
We implemented a procedure to classify the brain activity corresponding to rest and movement execution, or to rest and movement attempt (the procedures were applied separately for the healthy and the paretic hand) following our previous developments (López-Larraz et al., 2017a, 2017b). Although the analysis was conducted offline, all the methodologies were applied in a pseudo-online manner (using sliding windows, causal filters and auto-regressive models), simulating a real-time setup. Fig. 1-B displays the flowchart with the steps of the movement execution/attempt detection algorithm.

We used a block-based N-fold cross validation strategy, where N corresponded to the number of blocks recorded for each patient (N varied across patients between 4 and 6 blocks). In each fold, one of the blocks was kept apart for testing, and the rest of the blocks were used as training dataset. When the artifact rejection methods were applied, they were only applied to the training datasets. For the EOG artifact removal, the coefficients for the regression were computed using the training data only and applied posteriorly to the test trials, simulating an online execution.

With this procedure, we simulated different scenarios in which we process the data for training the BMI with different artifact rejection procedures and observe the effects on performance. The test trials with artifacts were not rejected; firstly, to simulate a real-time BMI use in which test artifacts cannot be predicted, and secondly, to have a fixed and unbiased test dataset for all the artifact rejection methods. Notice that all the proposed methods can be applied in real-time during the BMI operation to detect the artifacts in the test trials and, for instance, stop the feedback if an artifact is detected. With our approach, we assume that training the BMI with clean data is sufficient to characterize the brain activity of interest, and that therefore, the presence of those artifacts in the test trials should not bias the performance.
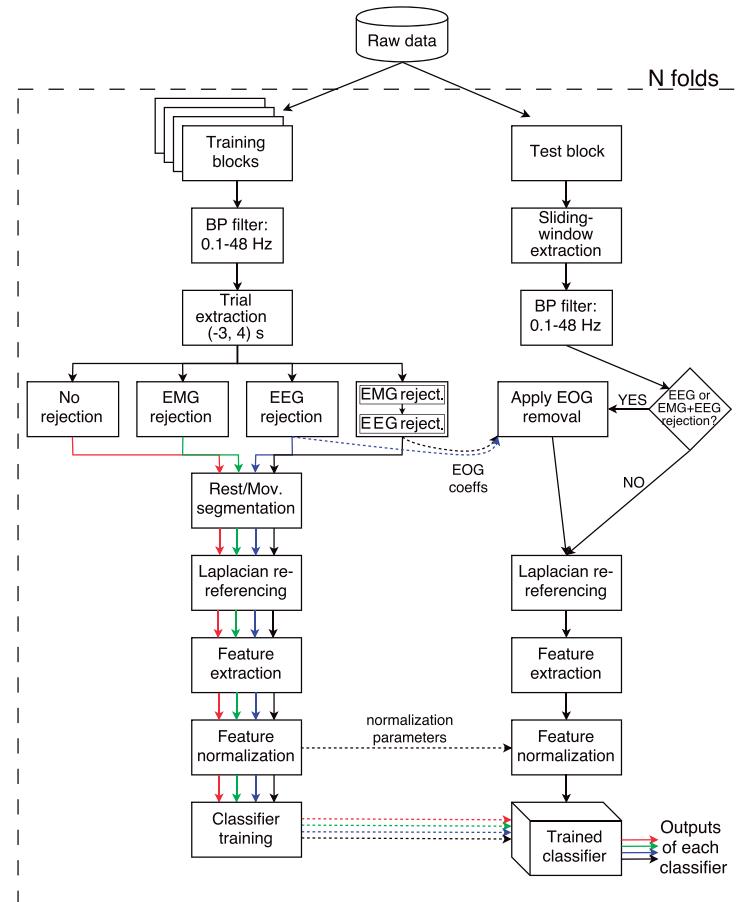
Fig. 1. Flowchart with the steps of each analysis. A) Steps for the quantification of cortical activity during the movement execution/attempt. The whole set of trials is processed four times (i.e., with each of the artifact rejection methods and without artifact rejection) and the cortical activity is estimated for each of the four methods. Notice that this procedure is performed separately for the movement executions with the healthy hand and the movement attempts with the paretic hand. B) Steps for the pseudo-online classification of movement execution/attepmt. The set of trials considered for training is processed four times (i.e., with each of the artifact rejection methods and without artifact rejection) and the four resulting training datasets are used to calibrate four classifiers. The test data is validated simulating an online processing, where parameters calculated in the training dataset are applied to the test set (e.g., EOG coefficients and normalization parameters). This scheme is performed as a N-fold cross validation, where N is the number of blocks recorded for each patient. Notice that this procedure is performed separately for the movement executions with the healthy hand and the movement attempts with the paretic hand.

2.6.2. Feature extraction

The 7-s trials (from -3 to $+4$ s with respect to the movement cue) were re-referenced using small Laplacian derivations (Hjorth, 1975). Unless otherwise specified, the BMI was trained with the activity of the electrodes placed on the contralateral hemisphere to the involved limb only: i.e., C3, CP3 and P3 if the right hand was involved; C4, CP4, P4 if the left hand was involved. Only those electrodes and their neighbors (used for the Laplacian) were considered for the artifact rejection.

We used one-second time windows to extract examples of EEG activity corresponding to resting state and to movement (execution or attempt). The examples of the rest class were extracted from the time interval $[-2, 0]$ s, and for the movement class they were extracted from the interval $[1, 3]$ s (since the reaction time in these patients may be slow (Yilmaz et al., 2015)), using a sliding step of 0.25 s in both cases (i.e., 5 windows of each class extracted from each trial). For each one-second window, the average power in the alpha ($[7–13]$ Hz) and the beta ($[14–30]$ Hz) frequency bands was computed for each of the three contralateral electrodes (i.e., the feature vector of each one-second window included 6 values). The power spectral density was computed using an order-20 autoregressive model, with a frequency resolution of 1 Hz, based on the Burg algorithm (Burg, 1975). The feature vectors of the training dataset were normalized to have zero mean and unit

variance. The normalization parameters (i.e., distribution mean and variance) were stored and applied to the test set in the pseudo-online validation of the BMI.

We also aimed at understanding how the artifacts can affect the features (i.e., the frequency bands) and the electrodes (i.e., the cortical positions) used to configure the BMI. Therefore, we repeated the process described above after varying the following parameters. Firstly, we evaluated the classification by using features of the alpha band only or the beta band only. In these cases, only 3 features were included in the feature vector: 1 frequency band for 3 electrodes. Secondly, we trained the classifier using the EEG electrodes from both hemispheres (i.e., contra- and ipsilateral to the moving limb). In this case, 12 features integrated the feature vectors (i.e., 2 frequency bands for 6 electrodes), and the six electrodes and their neighbors were taken into account for the artifact rejection.

A linear discriminant analysis (LDA) and a support vector machine (SVM) with a radial basis function kernel were evaluated as representative examples of linear and nonlinear classifiers (Lotte et al., 2007). The comparison between a linear and a non-linear classifier can provide relevant information to understand how they behave with data highly contaminated by artifacts. A linear classifier will trace the hyperplane that best separates between the data distributions of rest and
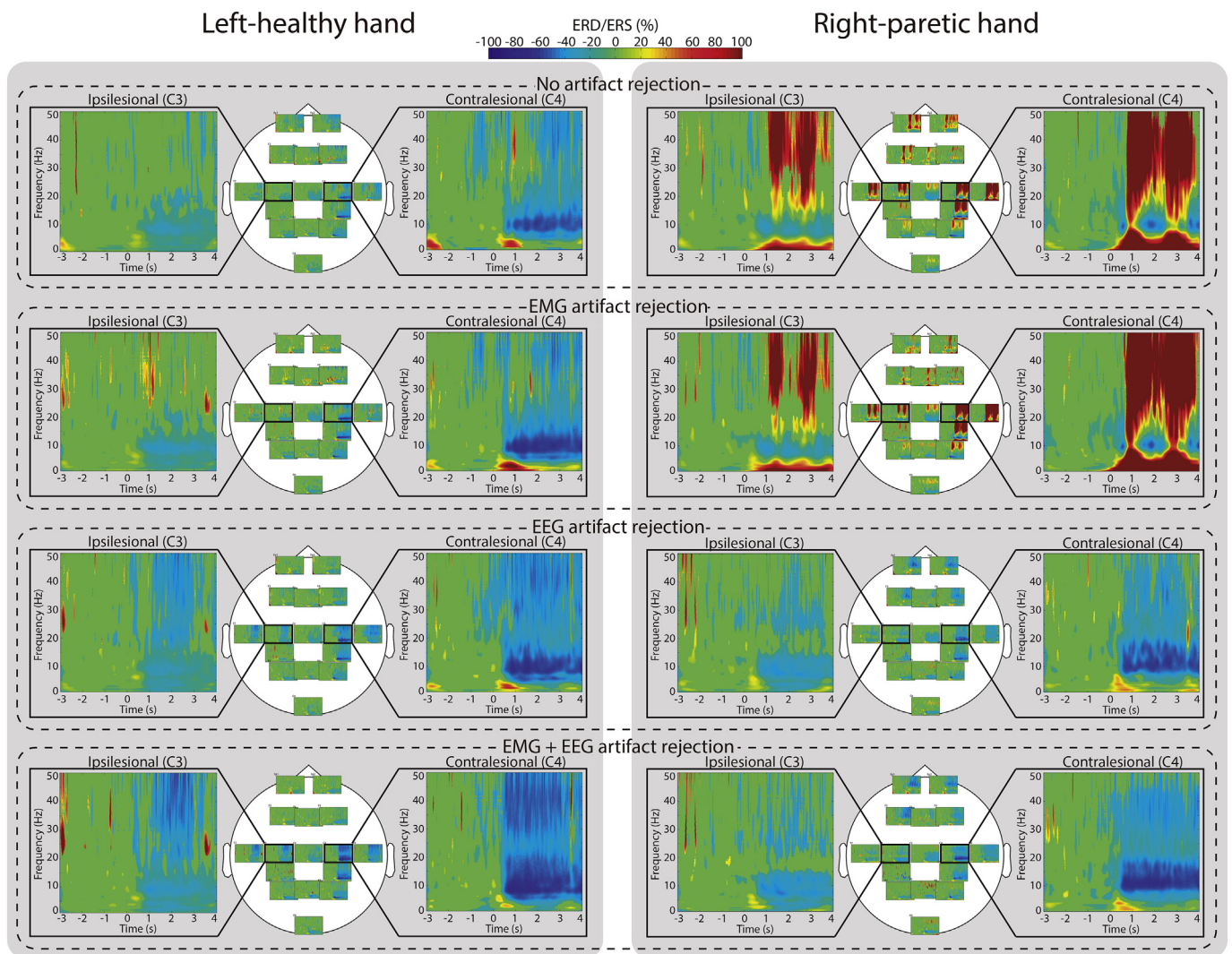
Left-healthy hand   Right-paretic hand

ERD/ERS (%)
-100 -80 -60 -40 -20 0 20 40 60 80 100

Fig. 2. Estimated cortical activation with each of the artifact rejection methods. The time-frequency maps represent the event-related (de) synchronization (ERS/ERD), averaged for all the patients, for each of the artifact rejection methods. Notice that the lateralized cortical positions of patients with the stroke in the right hemisphere are swapped, simulating that all the patients have the stroke in the left hemisphere. The percentage of ERS/ERD is calculated with respect to the resting baseline $[-2.5, -1]$ s. The left gray area corresponds to the movements of the healthy (left) hand, while the right gray area corresponds to the attempts of movement of the paretic (right) hand. Each of the four rows indicates one of the artifact rejection methods, encircled by dashed panels. The heads depict the ERD activity of each of the 16 EEG electrodes, averaged for all the patients. The activity of the left (i.e., ipsilesional) and right (i.e., contralesional) hemispheres is detailed by zooming the activity of C3 and C4 channels, respectively. Blue color indicates desynchronization, while red color represents synchronization with respect to the resting baseline. The artifact rejection methods, especially the ones based on EEG and EMG + EEG, reduce the influence of artifacts that cause the appearance of alpha and beta synchronization (i.e., ERS) during movement attempts, and enhance the ERD magnitude. (For interpretation of the references to color in this figure legend, the reader is referred to the web version of this article.).

movement. On the other hand, a non-linear classifier might be able to draw complex boundaries and learn both the artifacts (higher power with respect to rest) and the ERD activity (lower power with respect to rest), distinguishing them from the rest and providing higher accuracies.

2.6.3. Classification

The test blocks were classified simulating an online scenario. A one-second sliding window was applied from -3 to $+4$ s on each trial (notice that the first output was thus generated at $t = -2$ s), with the classifier generating an output every 20 ms.

The performance of the movement execution/attempt classifier was quantified in terms of average decoding accuracy, computed as the mean between the true positive rate (TPR) and the true negative rate (TNR). The TPR measures the success of the classifier during the movement period, which was considered the time interval $[1, 4]$ s. The

TNR measures the success of the classifier during the rest period, considered as the interval $[-2, 0]$ s.

2.7. Statistical analysis

Statistical analyses were performed to test if the different artifact rejection methods had a significant influence on the electrophysiological activity and on the performance of the classifier. We used the Friedman's test for non-Gaussian data with repeated measures (i.e., within subject comparisons), considering the artifact rejection method as factor, and the cortical activity (i.e., ERD in C3 or C4) or the decoding accuracy as dependent variables. Paired post-hoc comparisons were performed using the Wilcoxon signed-rank test to analyze significant differences between pairs. False discovery rate (FDR) correction was applied to control for the multiple comparisons, and statistical significance was considered when corrected p-values were smaller than

0.05. Correlation between the percentage of discarded trials and other clinical/demographic/performance variables was studied using Spearman's correlation coefficient.

3. Results

The average number of trials discarded for each patient by each artifact rejection method varied significantly between the healthy and the paretic limb (Wilcoxon signed-rank test, $p < .05$ for the three methods after FDR correction). For the movements of the healthy hand, $29.7 \pm 21.7\%$ of the trials were discarded if the EMG rejection was applied, $40.4 \pm 12.5\%$ for the EEG rejection, and $59.2 \pm 15.9\%$ for the EMG + EEG rejection. For the movement attempts of the paretic hand, the percentages of discarded trials were $39.2 \pm 20.3\%$ for the EMG rejection, $49.2 \pm 20.6\%$ for the EEG rejection, and $69.5 \pm 16.08\%$ for the EMG + EEG rejection. The number of discarded trials did not correlate significantly with any of the clinical and demographic data of the patients: i.e., gender, age, time since stroke, lesion side, location of the stroke, lesion volume and Fugl-Meyer score (Spearman correlation, $p > .05$ for the three methods and all the variables after FDR correction).

3.1. Quantification of cortical activity

3.1.1. Effect of artifact rejection on ERS/ERD

To facilitate visualization, we rearranged the EEG data to simulate that all the patients had the stroke in the left hemisphere. The lateralized cortical positions of patients with the stroke in the right hemisphere were flipped about the midline. Therefore, in subsequent analyses and figures, the left arm is always considered the healthy one, while the right arm is always considered the paretic one. Likewise, the left hemisphere of the motor cortex (represented by C3 cortical position) was always the ipsilesional area, while the right hemisphere (represented by C4 cortical position) corresponded to the contralesional area.

Fig. 2 compares the estimated brain activation after applying each of the artifact rejection methods. The time-frequency maps with the event-related (de) synchronization patterns are shown for the movement of the healthy hand (left) and for the movement attempt of the paretic hand (right). As can be seen, the most restrictive artifact rejection (based on EMG + EEG; bottom panels of the figure) clearly enhances the alpha and beta ERD in both hemispheres (i.e., ipsilesional or contralesional), regardless of the role they play with respect to the hand asked to move (i.e., contralateral or ipsilateral). On average for the group of patients, the contralesional electrodes showed stronger activation than the ipsilesional electrodes. Even when the patients attempted to move their paretic hand, the contralesional (i.e., ipsilateral) hemisphere was more active than the ipsilesional (i.e., contralateral) hemisphere. This may be explained by the fact that there were more patients with lesions involving the motor cortex, and these patients do not generally show a significant activation of the ipsilesional hemisphere during movement attempts but they activate the contralesional hemisphere (Luft et al., 2004; Park et al., 2016).

Fig. 3 illustrates the differences in alpha and beta ERD according to the artifact rejection method applied, and a summary of the statistic comparisons performed. For the movements of the healthy hand (Fig. 3, left panel), we first analyzed the ERD of the contralateral (i.e., contralesional; C4 electrode) hemisphere. There was a significant effect of the artifact rejection method on alpha ERD magnitude ($\chi^2(3) = 11.48$; $p = .009$), with a significant difference in the post-hoc comparisons between no artifact rejection and EMG + EEG rejection ($p = .048$); as well as an effect on the beta ERD magnitude ($\chi^2(3) = 19.06$; $p = .0003$), with significant differences in the post-hoc comparisons between no artifact rejection and EMG + EEG rejection ($p = .029$) and between EMG rejection and EMG + EEG rejection ($p = .004$). For the ipsilateral hemisphere to the moved healthy hand (i.e., ipsilesional; C3

electrode), the effect on alpha ERD was not significant ($\chi^2(3) = 7.80$; $p = .0503$), although it was for beta ERD ($\chi^2(3) = 7.95$; $p = .047$), with significant differences in the post-hoc comparisons between EMG rejection and EEG rejection ($p = .003$) and between EMG rejection and EMG + EEG rejection ($p = .014$).

For the attempts of movement of the paretic hand (Fig. 3, right panel), we followed the same procedure. In the contralateral (i.e., ipsilesional; C3 electrode) hemisphere, there was a significant effect of the artifact rejection method on alpha ERD magnitude ($\chi^2(3) = 14.52$; $p = .002$), with a significant difference in the post-hoc comparisons between no artifact rejection and EMG + EEG rejection ($p = .0007$) and between EMG rejection and EMG + EEG rejection ($p = .007$); similarly, there was a significant effect on the beta ERD magnitude ($\chi^2(3) = 11.92$; $p = .008$), with significant differences between no artifact rejection and EEG rejection ($p = .028$), between EMG rejection and EEG rejection ($p = .004$), and between EMG rejection and EMG + EEG rejection ($p = .0009$). For the ipsilateral hemisphere (i.e., contralesional; C4 electrode), the effect on alpha ERD was not significant ($\chi^2(3) = 5.00$; $p = .17$), despite the mean differences were higher than for the contralateral hemisphere (compare upper-left and -right plots of the right panel in Fig. 3); whilst for the beta ERD it was significant ($\chi^2(3) = 8.60$; $p = .035$), although none of the post-hoc comparisons were significant after correction.

3.1.2. Influence of each component of the EEG artifact rejection

We also studied the influence of each of the three components of the EEG artifact rejection procedure on the ERD: i.e., EOG removal, motion artifact rejection (based on low frequencies—LowFreq), and muscle artifact rejection (based on high frequencies—HighFreq); and compared them with the combination of the three of them (i.e., EEG rejection). In Fig. 4, we show the alpha and beta ERD elicited by the movement of the healthy hand and the movement attempt of the paretic hand in the contralateral hemisphere. For simplicity, the statistical results reported below correspond to the contralateral hemisphere to the involved limb. The results of the ipsilateral hemisphere are summarized in Supplementary Fig. 2.

For the healthy hand (Fig. 4, left panel), there were no differences between the four compared methods on alpha ERD ($\chi^2(3) = 7.36$; $p = .061$), but there were significant differences on beta ERD ($\chi^2(3) = 10.09$; $p = .018$), with significant differences between EEG rejection and EOG removal ($p = .046$), and between EOG removal and HighFreq rejection ($p = .017$). For the paretic hand (Fig. 4, right panel), there were significant differences both on alpha ERD ($\chi^2(3) = 9.80$; $p = .020$), with significant differences between EEG rejection and EOG removal ($p = .043$), and between EOG removal and HighFreq rejection ($p = .004$); as well as on beta ERD ($\chi^2(3) = 14.16$; $p = .003$), with significant differences between EEG rejection and EOG removal ($p = .018$), between EEG rejection and LowFreq rejection ($p = .005$), between EOG removal and HighFreq rejection ($p = .032$), and between LowFreq rejection and HighFreq rejection ($p = .047$).

3.2. Movement detection

3.2.1. Effects of artifact rejection

Fig. 5 shows the average results for the detection of movement execution and attempt based on the linear classifier (LDA) combining alpha and beta features extracted over the contralateral motor cortex. The figure displays the performance of the classifiers, indicating the percentage of outputs that are classified as movement (or movement attempt) on each time instant (i.e., this value should be low in the rest periods and high in the movement periods). We considered this configuration of classifier and feature extraction procedure as the reference for posterior comparisons. For the healthy hand (Fig. 5-left), there were no significant differences in accuracy between the four methods to process the artifacts ($\chi^2(3) = 1.71$; $p = .63$). For the paretic hand (Fig. 5-right), the different artifact rejection methods led to significantly
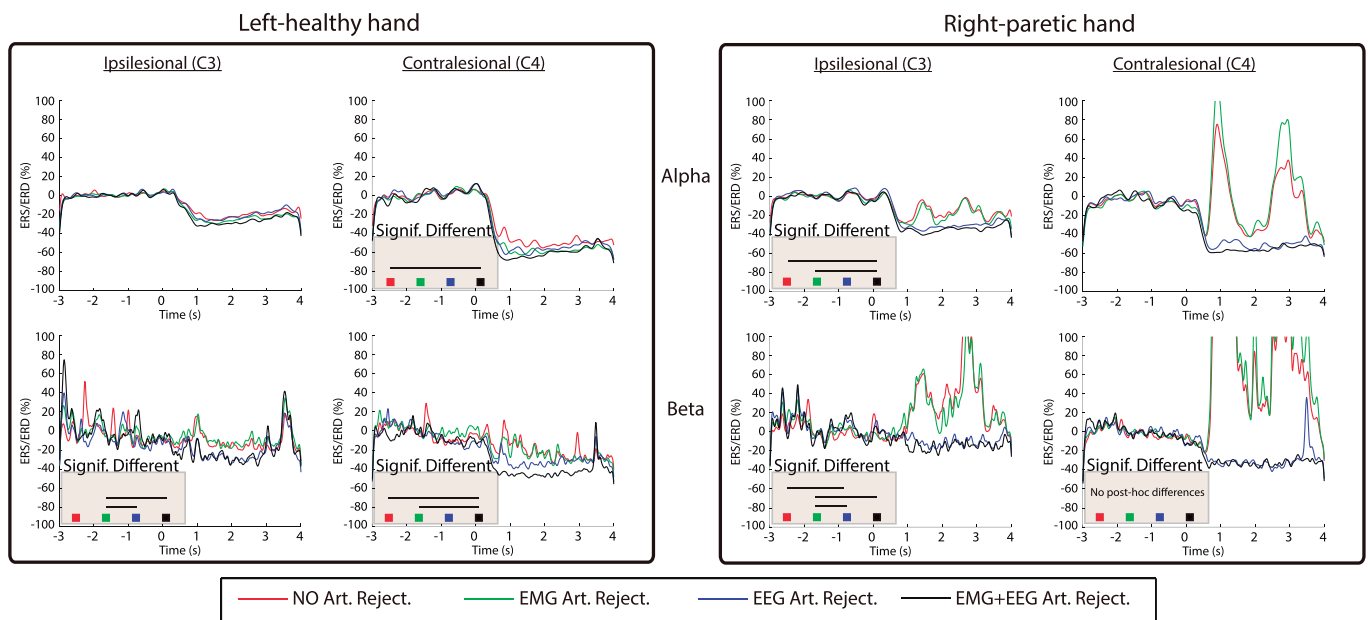
Fig. 3. Temporal evolvement of ERS/ERD in alpha (i.e., [7–13] Hz) and beta (i.e., [14–30] Hz) frequencies for the four artifact processing methods. Notice that the lateralized cortical positions of patients with the stroke in the right hemisphere are swapped, simulating that all the patients have the stroke in the left hemisphere. The percentage of ERS/ERD is calculated with respect to the resting baseline [−2.5, −1] s. The left panel corresponds to the movements of the healthy (left) hand, while the right panel corresponds to the attempts of movement of the paretic (right) hand. Within each panel, plots corresponding to the ipsilesional (left column) and contralesional (right column) hemispheres, and to alpha (upper row) and beta (bottom row) frequencies are included. Each plot shows the average ERD for each of the four artifact processing methods, indicated by the different colors. The results of the statistical analyses are indicated by the colored squares and horizontal lines in the shaded panel at the bottom-left of the plots. The presence of the "Signif. Different" panel indicates a significant effect of artifact rejection method on ERD magnitude (in the interval [0, 4] s), while the horizontal lines between pairs indicate the pairs of methods with significantly different ERD after correction for multiple comparisons.

different accuracies ($\chi^2(3) = 9.98$; $p = .019$). Post-hoc comparisons revealed that training the BMI without rejecting artifacts provided significantly higher decoding accuracies than rejecting artifacts based on EEG ($p = .022$) or based on EMG + EEG ($p = .044$).

When using a non-linear SVM classifier, the results were very similar to the ones observed with the linear classifier (see Supplementary Fig. 3). Paired comparisons between the four artifact processing methods for LDA and SVM were conducted (separately for each hand), showing no significant differences between the two classifiers in any case ($p > .05$). Therefore, all the subsequent analyses are based on an LDA-based classifier, since it is a simpler approach than the non-linear SVM.

3.2.2. Importance of the number and type of trials rejected

Discarding trials with artifacts from the training dataset led to average decreases in accuracy. One could think that this is due to the reduction of the number of observations used for training the classifier, and not to the fact that only the contaminated trials were rejected. To avoid this possible bias, we conducted two analyses.

Firstly, we measured if there is a significant correlation between the percentage of trials discarded by the different artifact rejection methods and the performance of the classifier. We used Spearman correlation with the data of all the subjects and artifact rejection methods and found no significant correlation neither for the healthy hand ($r = -0.11$; $p = .25$) nor for the paretic hand ($r = -0.15$; $p = .20$).

Secondly, we repeated the classification procedure but randomly eliminating from the training dataset the same number of trials that were rejected by the most restrictive method (i.e., based on EMG + EEG). This process was repeated 10 times for each fold of each patient. Fig. 6 shows the average results for this procedure with the reduced training dataset, compared with the training datasets without artifact rejection and with EMG + EEG artifact rejection (as displayed in Fig. 5). As for the analysis presented in the previous section, no

significant differences in performance were found between the three procedures for the healthy hand ($\chi^2(2) = 2.20$; $p = .33$). For the paretic hand, the rejection method had a significant effect on decoding accuracy ($\chi^2(2) = 8.11$; $p = .017$). Post-hoc comparisons showed that the EMG + EEG artifact rejection led to significantly lower performances than if no trials were rejected ($p = .017$), or if random trials were rejected from the training data ($p = .0015$); while not rejecting or rejecting random trials from the training dataset led to not significantly different results ($p > .05$).

3.2.3. Effects in the different frequency bands

When the linear classifier was trained with features of the alpha band only, the artifact rejection method had no significant influence on performance either for the healthy ($\chi^2(3) = 4.69$; $p = .20$) or for the paretic hand ($\chi^2(3) = 6.25$; $p = .10$). Similarly, for the classifier trained with the beta band only, no differences between artifact rejection methods in the healthy ($\chi^2(3) = 2.11$; $p = .55$) nor the paretic hand ($\chi^2(3) = 0.66$; $p = .88$) were found.

To measure possible interactions between these features and the artifact rejection method, we fitted a linear model, considering accuracy as dependent variable, and artifact rejection method (4 levels) and type of features (3 levels: alpha + beta, alpha, and beta) as factors. For the healthy hand, the type of features was a significant factor ($F_{2,11} = 3.84$, $p = .022$), with alpha + beta configuration providing significantly higher accuracies than alpha only ($p = .048$) and beta only ($p = .039$). For the paretic hand, again the type of features was a significant factor ($F_{2,11} = 21.15$, $p = 2.1 \times 10^{-9}$), with alpha + beta configuration providing significantly higher accuracies than alpha only ($p = .046$) and beta only ($p = 1.83 \times 10^{-9}$), and alpha being also significantly higher than beta ($p = 3.40 \times 10^{-5}$). Fig. 7 displays the performances of alpha, beta, and alpha + beta configurations for each of the four artifact processing methods when using the BMI for the healthy or paretic hand.
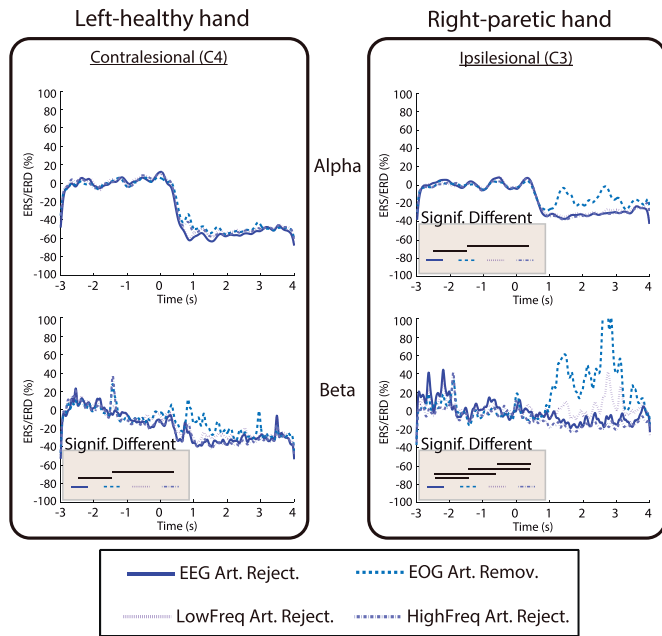
Left-healthy hand — Contralesional (C4)

Right-paretic hand — Ipsilesional (C3)

Alpha

Beta

Signif. Different

— EEG Art. Reject. ⋯⋯ EOG Art. Remov.
⋯ LowFreq Art. Reject. ⋯⋯ HighFreq Art. Reject.

Fig. 4. Temporal evolvement of ERS/ERD in alpha (i.e., [7–13] Hz) and beta (i.e., [14–30] Hz) frequencies for the EEG artifact rejection, and for each of its components separately. Notice that the lateralized cortical positions of patients with the stroke in the right hemisphere are swapped, simulating that all the patients have the stroke in the left hemisphere. The percentage of ERS/ERD is calculated with respect to the resting baseline $[-2.5, -1]$ s. The left panel corresponds to the movements of the healthy (left) hand, while the right panel corresponds to the attempts of movement of the paretic (right) hand. Within each panel, the activity of the contralateral hemisphere (i.e., contralesional for the healthy hand, and ipsilesional for the paretic hand) for alpha (upper row) and beta (bottom row) frequencies is shown. Each plot shows the average ERD for each of the four methods, indicated by the different colors and types of line. The results of the statistical analyses are indicated in the shaded panel at the bottom-left of the plots. The presence of the "Signif. Different" panel indicates a significant effect of artifact rejection method on ERD magnitude (in the interval $[0, 4]$ s), while the horizontal black lines between pairs indicate the pairs of methods with significantly different ERD after correction for multiple comparisons.

3.2.4. Influence of each EEG artifact rejection component

We also evaluated the effect that each of the three EEG artifact rejection components (namely EOG removal, motion artifacts rejection, and muscle artifacts rejection) had on decoding accuracy. Fig. 8 shows the results for the healthy and the paretic hand, comparing five
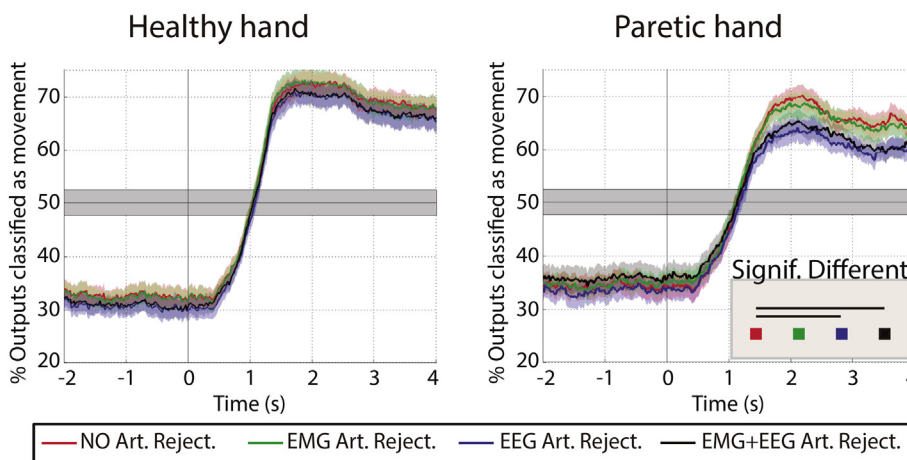
configurations: no artifact rejection, complete EEG artifact rejection (as reported in the previous results), EOG artifact removal only (EOG), motion artifact rejection only (based on low frequencies—LowFreq), muscle artifact rejection only (based on high frequencies—HighFreq). For the healthy hand, there were no significant differences in accuracy ($\chi^2(4) = 3.19$; $p = .52$). For the paretic hand, there was a significant effect on performance due to the EEG artifact rejection method ($\chi^2(4) = 16.24$; $p = .003$). Post-hoc comparisons revealed significant differences between no artifact rejection and the complete EEG artifact rejection (as already reported in 3.1.1; $p = .02$), between EEG rejection and EOG removal ($p = .0003$), between EEG and HighFreq rejection ($p = .004$), between EOG removal and LowFreq rejection ($p = .01$), and between EOG removal and HighFreq rejection ($p = .02$).

3.2.5. Effects when using both hemispheres

Providing contingent feedback associated to the activation of the contralateral (i.e., ipsilesional) hemisphere to the paralyzed limb during attempts of movement can lead to motor recovery in stroke patients (Ramos-Murguialday et al., 2013). Combining the activity of both hemispheres can lead to higher decoding accuracies than using only the ipsilesional one (López-Larraz et al., 2017b), despite there is no evidence supporting that this can also facilitate recovery.

We also investigated how the artifact rejection methods influenced the movement detection based on the activity of both hemispheres (Fig. 9). For this, both the artifact rejection and the feature extraction considered the electrodes placed on the left and right hemispheres. In this case, we found a significant effect of the artifact rejection method for the healthy hand ($\chi^2(3) = 22.85$; $p = 4.35 \times 10^{-5}$), with significant differences in performance between no artifact rejection and EMG + EEG artifact rejection ($p = .0007$), and between EMG and EMG + EEG artifact rejection ($p = .0015$). For the paretic hand, there were also significant differences in accuracy dependent on the rejection method ($\chi^2(3) = 33.00$; $p = 3.22 \times 10^{-7}$); paired comparisons showed significant differences in performance between no artifact rejection and EEG rejection ($p = .0001$), no artifact rejection and EMG + EEG rejection ($p = .0001$), EMG rejection and EEG rejection ($p = .011$), and EMG rejection and EMG + EEG rejection ($p = .0005$).

4. Discussion

EEG recordings are a relevant tool to study neural dynamics and to develop brain-machine interfaces (BMI) for motor rehabilitation of severely paralyzed stroke patients. The present study evidences the importance of appropriate methodologies to remove artifacts in EEG recordings of stroke patients to obtain accurate estimations of the motor brain activity. Firstly, removing the contaminations improves the
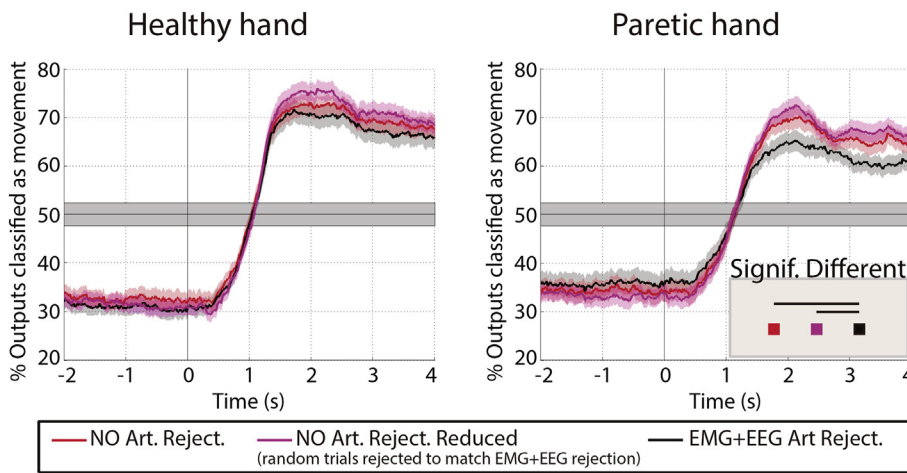

Healthy hand

Paretic hand

Signif. Different

— NO Art. Reject. — EMG Art. Reject. — EEG Art. Reject. — EMG+EEG Art. Reject.

Fig. 5. Average performance with a linear classifier (LDA-based) for the healthy (left) and the paretic (right) hands with each of the four artifact processing methods. On each panel, the lines represent the percentage of classifier outputs identified as movement, averaged for all the patients, and the shades indicate the standard error of the mean. Notice that the values before $t = 0$ correspond to false positives, while the values after $t = 0$ correspond to true positives. The shaded gray area indicates the confidence interval of the chance level (alpha = 0.01), computed on the basis of all the test trials, according to (Müller-Putz et al., 2008). The results of the statistical analyses are indicated by the colored squares and horizontal lines in the shaded panel at the bottom-right of the plots. The presence of the "Signif. Different" panel indicates a significant effect of artifact rejection method on the average BMI accuracy, while the horizontal lines between pairs indicate the pairs of methods with significantly different accuracy after correction for multiple comparisons.

Fig. 6. Average performance for the healthy (left) and the paretic (right) hands analyzing the influence of the number of trials rejected from the training dataset. On each panel, the lines represent the percentage of classifier outputs identified as movement, averaged for all the patients, and the shades indicate the standard error of the mean. Notice that the values before $t = 0$ correspond to false positives, while the values after $t = 0$ correspond to true positives. The shaded gray area indicates the confidence interval of the chance level (alpha = 0.01), computed on the basis of all the test trials, according to (Müller-Putz et al., 2008). The results of the statistical analyses are indicated in the shaded panel at the bottom-right of the plots. The presence of the "Signif. Different" panel indicates a significant effect of the method on the average BMI accuracy, while the horizontal lines between pairs indicate the pairs of methods with significantly different accuracy after correction for multiple comparisons.

quantification of the EEG-cortical activation during motor tasks. Secondly, when this activity is classified by a BMI to detect movement (or movement attempt), artifacts can cause an optimistic bias in the performance. This implies that training a BMI with a dataset not properly cleaned from artifacts can weaken the link that associates brain activation and proprioceptive feedback, which is hypothesized to be key to promote motor recovery (Ramos-Murguialday et al., 2013).

4.1. Methods for identifying and rejecting the artifacts

A large variety of methodologies can be applied to try to minimize the influence of artifacts on EEG data (Croft and Barry, 2000; Muthukumaraswamy, 2013; Urigüen and Garcia-Zapirain, 2015). Several methods allow removing (i.e., correcting) certain types of artifacts and reconstructing the EEG signals after cleaning the undesired components. These methods are especially useful for removing eye contaminations, since they are easy to be characterized, captured and filtered (Urigüen and Garcia-Zapirain, 2015). Among these methods, linear regression and independent component analysis (ICA) have been proven as the most efficient ones to remove ocular artifacts (Klados et al., 2009; Kobler et al., 2017; Schlögl et al., 2007; Urigüen and Garcia-Zapirain, 2015); although there is certain controversy about how the use of ICA may introduce additional sources of variance to the EEG and negatively impact the signals of interest (Pontifex et al., 2016).

However, for muscle and motion artifacts, these techniques may not be so effective. On the one hand, linear regression and adaptive filtering require a reference signal (as for instance, the EOG activity), which is hardly available for body motions and for all the muscles that may contaminate the EEG (e.g., shoulder, neck and cranial muscles) (Urigüen and Garcia-Zapirain, 2015). On the other hand, despite ICA has also been used in offline analyses to clean artifactual components such as motion and muscle artifacts, it has two limitations that hinder their direct applicability to BMI-based rehabilitation therapies for patients with paralysis. Firstly, it is not trivial to decipher what components correspond to artifacts, and for this reason they are generally selected by visual inspection (Pereira et al., 2017; Seeber et al., 2016; Wagner et al., 2016), which makes it unpractical for a BMI therapy. Secondly, when patients try to move their paralyzed limb, these types of artifacts can be highly correlated with the brain activity of interest, which can reduce the capacity of the algorithm to remove the contaminations. For these reasons, statistical methods have been proposed as a simple way of rejecting outlier values with respect to a threshold on certain signal descriptors (e.g., amplitude, variance, power in a frequency band, etc.) (López-Larraz et al., 2014; Nolan et al., 2010). This allows analyzing the EEG signals after removing the influence of motion and muscle artifacts, among others.

We used automated state-of-the-art methods to minimize the influence of artifacts. The types of artifacts that we tried to detect and
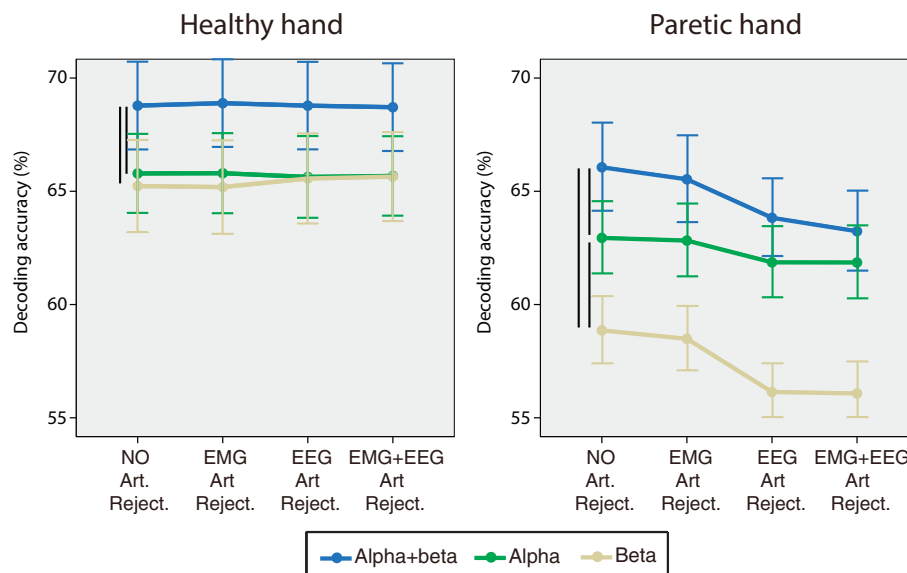

Fig. 7. Interaction plots studying the effects on decoding accuracy of the artifact rejection methods and the frequency bands used to extract the features for the BMI classifier. Only the factor "type of feature" was significant for the linear model. The vertical black bars denote statistical significance between pairs of types of features after correction for multiple comparisons. The whiskers on each point show the standard error of the mean.
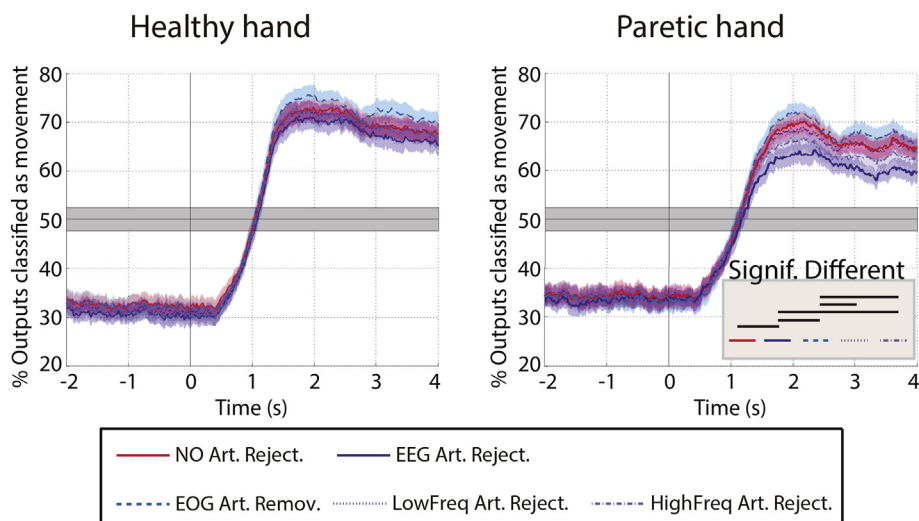
Fig. 8. Average performance for the healthy (left) and the paretic (right) hands analyzing the influence of the different components of the EEG artifact rejection. On each panel, the lines represent the percentage of classifier outputs identified as movement, averaged for all the patients, and the shades indicate the standard error of the mean. Notice that the values before $t = 0$ correspond to false positives, while the values after $t = 0$ correspond to true positives. The shaded gray area indicates the confidence interval of the chance level (alpha = 0.01), computed on the basis of all the test trials, according to (Müller-Putz et al., 2008). The results of the statistical analyses are indicated in the shaded panel at the bottom-right of the plots. The presence of the "Signif. Different" panel indicates a significant effect of the method on the average BMI accuracy, while the horizontal black lines between pairs indicate the pairs of methods with significantly different accuracy after correction for multiple comparisons.

eliminate were: 1) undesired movements (monitoring EMG to avoid trials with movements during the baseline intervals or involving the limb that was asked to keep relaxed); 2) eye contaminations; 3) motion artifacts; and 4) muscle artifacts. Eye contaminations were removed with a linear regression (Schlögl et al., 2007), while the other three types of artifacts were identified with a trial-based statistical thresholding and rejected. The rejection based on EMG activity identified the trials with inappropriate movements, which, if not discarded, might affect the quantification of the cortical activity (Ramos-Murguialday et al., 2010). The rejection based on EEG activity, and especially the one based on high frequencies (i.e., identification of muscle artifacts) was the one that contributed the most to enhance the estimated cortical activation, measured as the ERD. Although we cannot guarantee that the methods we used identified and rejected all the artifacts in the signals, they are sufficient to investigate if and to what extent the artifacts influenced the measured brain activity.

It is not trivial to determine what the optimal procedure is to eliminate artifacts from EEG activity. In environments where external interferences are introduced, for instance, by closed-loop electric or magnetic stimulation, ad-hoc studies should be conducted to find the best strategy that minimizes their influence (Hoffmann et al., 2011; Insausti-Delgado et al., 2017; Walter et al., 2012). Physiological artifacts have different origins, and different procedures are required to minimize them. For instance, in the context of the present study with severely paralyzed stroke patients, muscle artifacts were the ones affecting to a higher extent both ERD magnitude and BMI performance.

Therefore, the rejection based on high frequencies of the EEG had the strongest influence. Rejection based on low frequency EEG and electrooculographic activity had a smaller impact on ERD and BMI performance. This is probably due to the fact that we based our analyses on alpha and beta frequency bands (i.e., [7–30] Hz), but also because the patients performed a grasping task, which elicits less eye and head movements, in contrast to other movements such as reaching or walking (Ibáñez et al., 2014; López-Larraz et al., 2016; Shiman et al., 2017; Velu and de Sa, 2013). Therefore, the methodology employed to remove contaminations from EEG activity should always be carefully designed according to the aim of the study and the particularities of the protocol to be conducted.

4.2. Influence on the quantification of cortical activity

We showed that rejecting trials with artifacts helps to capture more accurately the brain activation during motor execution and motor attempt. The values of the ERD were always higher in absolute value (since the ERD is measured with negative values (Graimann and Pfurtscheller, 2006)) using the most restrictive artifact rejection method (i.e., based on EMG + EEG activity). The rejection of artifacts revealed a stronger contralesional activation during the attempt of movement of the hand, which could not be appreciated without removing artifacts (cf. Fig. 2). This contralesional activation is a known phenomenon that has already been described in fMRI studies (Grefkes et al., 2008; Rehme et al., 2011; Ward et al., 2003). Proper cleaning of
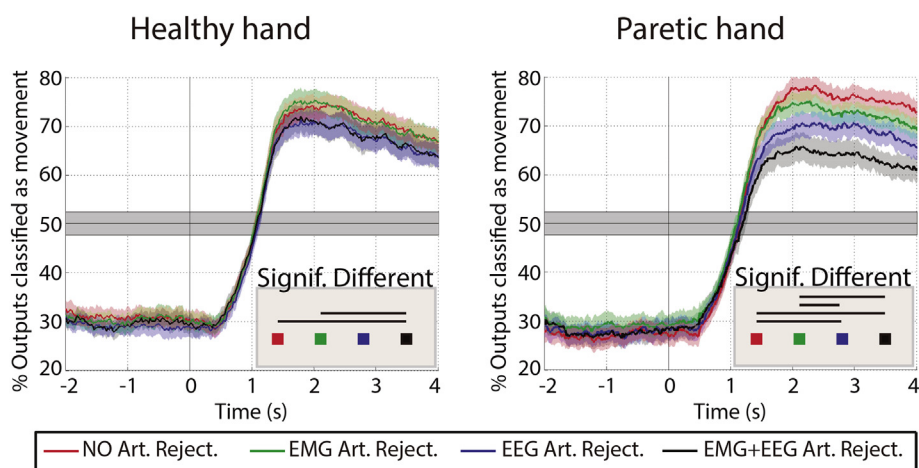

Fig. 9. Average performance for the healthy (left) and the paretic (right) hands when the BMI was trained with the activity of both hemishperes. On each panel, the lines represent the percentage of classifier outputs identified as movement, averaged for all the patients, and the shades indicate the standard error of the mean. Notice that the values before $t = 0$ correspond to false positives, while the values after $t = 0$ correspond to true positives. The shaded gray area indicates the confidence interval of the chance level (alpha = 0.01), computed on the basis of all the test trials, according to (Müller-Putz et al., 2008). The results of the statistical analyses are indicated in the shaded panel at the bottom-right of the plots. The presence of the "Signif. Different" panel indicates a significant effect of the method on the average BMI accuracy, while the horizontal black lines between pairs indicate the pairs of methods with significantly different accuracy after correction

for multiple comparisons.

EEG contaminations is a crucial step for future analyses that aim at characterizing specific brain activation patterns after stroke. Further research could be conducted to investigate how EEG activity varies according to the location of the stroke, revealing which brain structures contribute most to the magnitude of the ERD, and complementing previous fMRI studies (Luft et al., 2004).

Although artifacts also influenced the brain activity related to the movements of the healthy hand, the effect was more evident for the activity elicited during the movement attempts of the paretic hand. This probably reflects the fact that the attempts of movement with a paralyzed limb require extra efforts that generate more frequent and larger artifacts (e.g., head and eye movements or contractions of neck and cranial muscles) and compensatory movements with other body parts. In general, the beta band was more affected than alpha, presumably due to its proximity to the spectral bandwidth of muscle activity (Muthukumaraswamy, 2013). This reveals why the EEG artifact rejection based on high frequencies contributed the most to cleaning these artifacts (cf. Fig. 4).

The artifact rejection method based on EMG activity discarded almost 40% of the trials of the paretic hand and 30% of the healthy hand. Interestingly, it never improved the measurements of cortical activity compared to not rejecting artifacts. This suggests that the undesired movement components detected by the EMG rejection may not significantly influence the estimated brain activity. However, this result should be interpreted with caution. The fact that the estimations of cortical activation did not change significantly after our EMG rejection does not imply that compensatory movements do not affect the activity. The subjects should always be carefully instructed to avoid compensatory activity with other limbs, and their compliance with the task should be monitored. Furthermore, certain tasks can be more prone to cause other limbs to move during the unsuccessful attempts; for instance, the task in this study (i.e., grasping) may require less compensation with the trunk or with the healthy arm than a reaching task. If those contaminated trials are not rejected, their processing can result in an inaccurate estimation of cortical activation, not corresponding to the task that is under investigation (Pineda et al., 2000), which can bias the conclusions or hamper the BMI-based rehabilitation therapy. Still, we observed that the combination of EMG and EEG rejection led to slightly higher values of brain activation, although the differences were not statistically significant (see, for instance, how in the right plots of the left panel of Fig. 3, the black line is always more negative than the blue line during the movement period; or how in Fig. 2, the fourth row displays a stronger activation than the third row). For these reasons, we would recommend researchers to carefully analyze their datasets and identify possible contaminations that may be cleaned by the proposed EMG rejection: i.e., discarding those trials with muscular activation during the rest intervals, or activation of the other limbs.

4.3. Implications for brain machine interfaces

The differences that we observed in the brain activity with the artifact rejection methods also translated into differences in BMI classification accuracy. We already demonstrated in a previous study that eliminating EOG, motion and muscle artifacts decreased, in general, the BMI performance (López-Larraz et al., 2017a). We confirmed those results and observed that additionally rejecting the trials with undesired movements (based on the EMG activity) did not change significantly the performance of the BMI classifier trained with the electrodes of the contralateral hemisphere only. Interestingly, when the BMI classifier relied on cortical information from both hemispheres, the differences between artifact rejection methods were larger, especially for the paretic limb. This is likely due to the higher degree of contamination that we found in the ipsilateral hemisphere during the attempts of movement. In addition, it has important implications for BMIs using the contralesional activity to detect movement attempts of stroke patients (Ang et al., 2015; Antelis et al., 2017; López-Larraz et al.,

2018a, 2017b; Ono et al., 2014; Tangwiriyasakul et al., 2014a), since the training data should be more carefully cleaned to avoid biasing the classifier with artifacts.

We did not find any evidence supporting that linear or non-linear classifiers are more prone to being contaminated with artifacts, and very similar performances were obtained when using LDA- or SVM-based classifiers. This result supports the idea that in this type of BMI for movement detection, the features and processing of the data have a stronger influence than the classifier itself (Bashashati et al., 2015). In fact, we could observe that combining features based on alpha and beta frequencies to train the BMI classifier had a significantly positive impact on performance.

4.4. Implications for clinical practice

Brain machine interfaces have demonstrated their efficacy for rehabilitation after paralysis (Ang et al., 2015; Biasiucci et al., 2018; Donati et al., 2016; Ono et al., 2014; Pichiorri et al., 2015; Ramos-Murguialday et al., 2013; Trincado-Alonso et al., 2018). However, this technology is still in a preliminary stage, and there is a great margin for investigation and improvement before it becomes one standard tool in the portfolio of clinical treatments for motor rehabilitation (Asín Prieto et al., 2014; López-Larraz et al., 2018b). The results presented in this study demonstrate, on the one hand, that rejecting trials with artifacts from the EEG datasets helps to better quantify the brain activity of stroke patients during motor tasks; and on the other hand, that after rejecting the artifacts from the training datasets, the obtained BMI performances are lower. However, it detects significantly better the brain activity related to the motor task, guaranteeing a better link between brain and muscles, shown to be key for motor rehabilitation (Ramos-Murguialday et al., 2013). Therefore, for an actual BMI intervention, we would recommend cleaning the training datasets with all the available information; meaning that EEG rejection should necessarily be conducted, while EMG rejection could be included or not depending on the protocol and the availability of EMG signals.

We have shown in a previous study that drops in performance of EEG-based movement intention detection might be due to the presence of artifacts in the test data (López-Larraz et al., 2017a). This suggests that when artifacts are removed from the training dataset, the classifier does not learn those patterns, and therefore avoids their possible bias in the BMI control, since it is not able to recognize them as relevant information. The important question that arises is: What is the influence that this drop in performance has in rehabilitation? To date, we can only speculate that it is not the general BMI performance (as measured in this or in previous papers) the responsible for the success of the therapy. More specifically, we conjecture that it is the accurate and contingent link between the activation of the neuronal populations in the motor network and the peripheral feedback in the paralyzed limbs what supports recovery (Jackson and Zimmermann, 2012). As shown in this paper, artifact rejection is an efficient way to improve the characterization of the brain activity responsible for motor commands. Therefore, it should be able to improve the contingent association between brain and muscles and intensify the neuroplastic and rehabilitative effects of BMI-based therapies.

4.5. Limitations and perspectives

In this study, we focused on quantifying the brain activation by means of the event-related desynchronization/synchronization (ERD/ERS) of the alpha and beta rhythms. These EEG correlates of movement are the most widely used in BMI rehabilitative therapies with stroke or SCI patients (Ang et al., 2015; Biasiucci et al., 2018; Donati et al., 2016; Ono et al., 2014; Pichiorri et al., 2015; Ramos-Murguialday et al., 2013). Other correlates, such as the movement-related cortical potentials (MRCP) have also been proposed for rehabilitative BMI systems, due to its good temporal precision (Mrachacz-Kersting et al., 2012;

Mrachacz-Kersting et al., 2016), that can facilitate Hebbian plasticity, and their capacity to encode information about different movements (Schwarz et al., 2018). However, MRCPs require asynchronous paradigms (i.e., no visual/auditory cues are used to guide the patients), since the use of cues reduces their amplitude (Savić et al., 2014), and they are more easily contaminated by motion artifacts (Castermans et al., 2014). Consequently, further research should evaluate the response of BMIs relying on these correlates in the presence of artifacts.

Despite we conducted the simulations of the BMI in a pseudo-online fashion, it was still an offline analysis that does not allow capturing the possible artifacts or influences that can appear during a real-time use of this type of systems. Our results help understanding how to process the EEG datasets before calibrating a BMI for being used in closed-loop rehabilitation. However, during the closed-loop operation, artifacts also occur. Some of them, such as the EOG contaminations, can be effectively filtered in real-time, while for other types of artifacts, automatized procedures for removal are not sufficiently precise. Our approach assumed that having a clean training dataset is enough to appropriately model the activity that we want to detect, so that in real-time, muscle and motion artifacts do not bias the BMI performance. However, notice that it may also be possible to implement an online system that detects the artifacts, based on the same procedures we presented here, and completely stops the feedback when contaminations are detected. For instance, a real-time detector of compensatory movements with other limbs may stop the movement of the rehabilitative device in a BMI therapy when the patient activates muscles that should remain relaxed (Wright et al., 2014).

The BMI design that we used was rather simple in terms of the feature extraction and the classification algorithms. We estimated the spectral power of the alpha and beta frequencies with an auto-regressive model and used a linear discriminant analysis as a classifier. There are several studies investigating how to optimize the feature processing and the classification algorithms (Bashashati et al., 2007, 2015; Brunner et al., 2011; López-Larraz et al., 2018a; Lotte et al., 2007), and therefore, our approach may not be the best available method in terms of classification accuracy. Our motivation for using this design was based on our previous work (Ramos-Murguialday et al., 2013), which proved the BMI rehabilitation efficacy (coupled with physiotherapy) of the contingent association between ipsilesional activity and peripheral feedback during movement attempts in stroke patients. We hypothesize that more advanced BMI methodologies (e.g., common-spatial patterns (Blankertz et al., 2008; Sannelli et al., 2016)) may lead to higher global performances, but still would be sensitive to the presence of artifacts in the training datasets, and this might result in a poorer rehabilitation efficacy. However, further research should be conducted to verify the response of other BMI designs with the presence or absence of artifacts in the data.

Conflicts of interest

The authors declare that there is no conflict of interest regarding the publication of this paper.

Acknowledgments

Appendix A. Supplementary data

Supplementary data to this article can be found online at https://doi.org/10.1016/j.nicl.2018.09.035.

References

Ang, K.K., Chua, K.S.G., Phua, K.S., Wang, C., Chin, Z.Y., Kuah, C.W.K., Low, W., Guan, C., 2015. A randomized controlled trial of EEG-based motor imagery brain-computer interface robotic rehabilitation for stroke. Clin. EEG Neurosci. 46, 310–320. https://doi.org/10.1177/1550059414522229.

Antelis, J.M., Montesano, L., Ramos-Murguialday, A., Birbaumer, N., Minguez, J., 2017. Decoding upper limb movement attempt from EEG measurements of the contralesional motor cortex in chronic stroke patients. IEEE Trans. Biomed. Eng. 64, 99–111. https://doi.org/10.1109/TBME.2016.2541084.

Asín Prieto, G., Cano-de-la-Cuerda, R., López-Larraz, E., Metrot, J., Molinari, M., Dokkum, L.E.H., 2014. Emerging perspectives in stroke rehabilitation. In: Pons, J.L., Torricelli, D. (Eds.), Emerging Therapies in Neurorehabilitation. Springer Berlin Heidelberg, Berlin, pp. 3–21. https://doi.org/10.1007/978-3-642-38556-8.

Bashashati, A., Fatourechi, M., Ward, R.K., Birch, G.E., 2007. A survey of signal processing algorithms in brain-computer interfaces based on electrical brain signals. J. Neural Eng. 4, R32–R57. https://doi.org/10.1088/1741-2560/4/2/R03.

Bashashati, H., Ward, R.K., Birch, G.E., Bashashati, A., 2015. Comparing different classifiers in sensory motor brain computer interfaces. PLoS One 10, e0129435. https://doi.org/10.1371/journal.pone.0129435.

Biasiucci, A., Leeb, R., Iturrate, I., Perdikis, S., Al-Khodairy, A., Corbet, T., Schnider, A., Schmidlin, T., Zhang, H., Bassolino, M., Viceic, D., Vuadens, P., Guggisberg, A.G., Millán, J. d R., 2018. Brain-actuated functional electrical stimulation elicits lasting arm motor recovery after stroke. Nat. Commun. 9, 2421. https://doi.org/10.1038/s41467-018-04673-z.

Blankertz, B., Tomioka, R., Lemm, S., 2008. Optimizing spatial filters for robust EEG single-trial analysis. IEEE Signal Process. Mag. 25, 41–56. https://doi.org/10.1109/MSP.2008.4408441.

Brunner, C., Billinger, M., Vidaurre, C., Neuper, C., 2011. A comparison of univariate, vector, bilinear autoregressive, and band power features for brain-computer interfaces. Med. Biol. Eng. Comput. 49, 1337–1346. https://doi.org/10.1007/s11517-011-0828-x.

Burg, J.P., 1975. Maximum Entropy Spectral Analysis, in: Proceedings of the 37th Annual International SEG Meeting.

Castermans, T., Duvinage, M., Cheron, G., Dutoit, T., 2014. About the cortical origin of the low-delta and high-gamma rhythms observed in EEG signals during treadmill walking. Neurosci. Lett. 561, 166–170. https://doi.org/10.1016/j.neulet.2013.12.059.

Chaudhary, U., Birbaumer, N., Ramos-Murguialday, A., 2016. Brain-computer interfaces for communication and rehabilitation. Nat. Rev. Neurol. 12, 513–525. https://doi.org/10.1038/nrneurol.2016.113.

Croft, R.J., Barry, R.J., 2000. Removal of ocular artifact from the EEG: a review. Neurophysiol. Clin. 30, 5–19. https://doi.org/10.1016/S0987-7053(00)00055-1.

Donati, A.R.C., Shokur, S., Morya, E., Campos, D.S.F., Moioli, R.C., Gitti, C.M., Augusto, P.B., Tripodi, S., Pires, C.G., Pereira, G.A., Brasil, F.L., Gallo, S., Lin, A.A., Takigami, A.K., Aratanha, M.A., Joshi, S., Bleuler, H., Cheng, G., Rudolph, A., Nicolelis, M.A.L., 2016. Long-term training with a brain-machine interface-based gait protocol induces partial neurological recovery in paraplegic patients. Sci. Rep. 6, 30383. https://doi.org/10.1038/srep30383.

Graimann, B., Pfurtscheller, G., 2006. Quantification and visualization of event-related changes in oscillatory brain activity in the time-frequency domain. Prog. Brain Res. 159, 79–97. https://doi.org/10.1016/S0079-6123(06)59006-5.

Grefkes, C., Nowak, D.A., Eickhoff, S.B., Dafotakis, M., Küst, J., Karbe, H., Fink, G.R., 2008. Cortical connectivity after subcortical stroke assessed with functional magnetic resonance imaging. Ann. Neurol. 63, 236–246. https://doi.org/10.1002/ana.21228.

Hammond, D.C., Gunkelman, J., 2001. The art of artifacting. Society for Neuronal Regulation.

Hjorth, B., 1975. An on-line transformation of EEG scalp potentials into orthogonal source derivations. Electroencephalogr. Clin. Neurophysiol. 39, 526–530. https://doi.org/10.1016/0013-4694(75)90056-5.

Hoffmann, U., Cho, W., Ramos-Murguialday, A., Keller, T., 2011. Detection and removal of stimulation artifacts in electroencephalogram recordings. In: 33rd Annual International Conference of the IEEE Engineering in Medicine and Biology Society (EMBC), pp. 7159–7162. https://doi.org/10.1109/IEMBS.2011.6091809.

Hortal, E., Planelles, D., Resquin, F., Climent, J.M., Azorin, J.M., Pons, J.L., 2015. Using a brain-machine interface to control a hybrid upper limb exoskeleton during rehabilitation of patients with neurological conditions. J. Neuroeng. Rehabil. 12, 92. https://doi.org/10.1186/s12984-015-0082-9.

Ibáñez, J., Serrano, J.I., del Castillo, M.D., Monge-Pereira, E., Molina-Rueda, F., Alguacil-Diego, I., Pons, J.L., 2014. Detection of the onset of upper-limb movements based on the combined analysis of changes in the sensorimotor rhythms and slow cortical potentials. J. Neural Eng. 11, 056009. https://doi.org/10.1088/1741-2560/11/5/056009.

Ibáñez, J., Monge-Pereira, E., Molina-Rueda, F., Serrano, J.I., Castillo, M.D., Cuesta-Gómez, A., Carratalá-Tejada, M., Cano-De-La-Cuerda, R., Alguacil-Diego, I.M., Miangolarra-Page, J.C., Pons, J.L., 2017. Low latency estimation of motor intentions to assist reaching movements along multiple sessions in chronic stroke patients: a feasibility study. Front. Neurosci. 11, 126. https://doi.org/10.3389/fnins.2017.00126.

Insausti-Delgado, A., López-Larraz, E., Bibián, C., Nishimura, Y., Birbaumer, N., Ramos-Murguialday, A., 2017. Influence of trans-spinal magnetic stimulation in electrophysiological recordings for closed-loop rehabilitative systems. In: 39th Annual International Conference of the IEEE Engineering in Medicine and Biology Society (EMBC), pp. 2518–2521. https://doi.org/10.1109/EMBC.2017.8037369.

Jackson, A., Zimmermann, J.B., 2012. Neural interfaces for the brain and spinal cord—restoring motor function. Nat. Rev. Neurol. 8, 690–699. https://doi.org/10.1038/nrneurol.2012.219.

Kaiser, V., Daly, I., Pichiorri, F., Mattia, D., Müller-Putz, G.R., Neuper, C., 2012. Relationship between electrical brain responses to motor imagery and motor impairment in stroke. Stroke 43, 2735–2740. https://doi.org/10.1161/STROKEAHA.112.665489.

Klados, M.A., Papadelis, C.L., Bamidis, P.D., 2009. REG-ICA: A new hybrid method for EOG artifact rejection. In: Final Program and Abstract Book -9th International Conference on Information Technology and Applications in Biomedicine, ITAB 2009, https://doi.org/10.1109/ITAB.2009.5394295.

Kline, J.E., Huang, H.J., Snyder, K.L., Ferris, D.P., 2015. Isolating gait-related movement artifacts in electroencephalography during human walking. J. Neural Eng. 12, 046022. https://doi.org/10.1088/1741-2560/12/4/046022.

Kobler, R.J., Sburlea, A.I., Müller-Putz, G.R., 2017. A comparison of ocular artifact removal methods for block design based electroencephalography experiments. In: Proceedings of the 7th Graz Brain-Computer Interface Conference, pp. 236–241. https://doi.org/10.3217/978-3-85125-533-1-44.

Lebedev, M.A., Nicolelis, M.A.L., 2017. Brain-machine interfaces: from basic science to neuroprostheses and neurorehabilitation. Physiol. Rev. 97, 767–837. https://doi.org/10.1152/physrev.00027.2016.

López-Larraz, E., Montesano, L., Gil-Agudo, Á., Minguez, J., 2014. Continuous decoding of movement intention of upper limb self-initiated analytic movements from pre-movement EEG correlates. J. Neuroeng. Rehabil. 11, 153. https://doi.org/10.1186/1743-0003-11-153.

López-Larraz, E., Montesano, L., Gil-Agudo, Á., Minguez, J., Oliviero, A., 2015. Evolution of EEG motor rhythms after spinal cord injury: a longitudinal study. PLoS One 10, e0131759. https://doi.org/10.1371/journal.pone.0131759.

López-Larraz, E., Trincado-Alonso, F., Rajasekaran, V., Del-Ama, A.J., Aranda, J., Minguez, J., Gil-Agudo, Á., Montesano, L., 2016. Control of an ambulatory exoskeleton with a brain-machine interface for spinal cord injury gait rehabilitation. Front. Neurosci. 10, 359. https://doi.org/10.3389/fnins.2016.00359.

López-Larraz, E., Bibián, C., Birbaumer, N., Ramos-Murguialday, A., 2017a. Influence of artifacts on movement intention decoding from EEG activity in severely paralyzed stroke patients. In: 15th International Conference on Rehabilitation Robotics (ICORR), pp. 901–906. https://doi.org/10.1109/ICORR.2017.8009363.

López-Larraz, E., Ray, A.M., Figueiredo, T.C., Bibián, C., Birbaumer, N., Ramos-Murguialday, A., 2017b. Stroke lesion location influences the decoding of movement intention from EEG. In: 39th Annual International Conference of the IEEE Engineering in Medicine and Biology Society (EMBC), pp. 3065–3068. https://doi.org/10.1109/EMBC.2017.8037504.

López-Larraz, E., Ibáñez, J., Trincado-Alonso, F., Monge-Pereira, E., Pons, J.L., Montesano, L., 2018a. Comparing recalibration strategies for electroencephalography-based decoders of movement intention in neurological patients with motor disability. Int. J. Neural Syst. 28, 1750060. https://doi.org/10.1142/S0129065717500605.

López-Larraz, E., Sarasola-Sanz, A., Irastorza-Landa, N., Birbaumer, N., Ramos-Murguialday, A., 2018b. Brain-machine interfaces for rehabilitation in stroke: a review. Neuro Rehabil. 43 (1), 77–97. https://doi.org/10.3233/NRE-172394.

Lotte, F., Congedo, M., Lécuyer, A., Lamarche, F., Arnaldi, B., 2007. A review of classification algorithms for EEG-based brain-computer interfaces. J. Neural Eng. 4, R1–R13. https://doi.org/10.1088/1741-2560/4/2/R01.

Luft, A.R., Waller, S., Forrester, L., Smith, G.V., Whitall, J., Macko, R.F., Schulz, J.B., Hanley, D.F., 2004. Lesion location alters brain activation in chronically impaired stroke survivors. NeuroImage 21, 924–935. https://doi.org/10.1016/j.neuroimage.2003.10.026.

Mrachacz-Kersting, N., Kristensen, S.R., Niazi, I.K., Farina, D., 2012. Precise temporal association between cortical potentials evoked by motor imagination and afference induces cortical plasticity. J. Physiol. 590, 1669–1682. https://doi.org/10.1113/jphysiol.2011.222851.

Mrachacz-Kersting, N., Jiang, N., Stevenson, A.J.T., Niazi, I.K., Kostic, V., Pavlovic, A., Radovanovic, S., Djuric-Jovicic, M., Agosta, F., Dremstrup, K., Farina, D., 2016. Efficient neuroplasticity induction in chronic stroke patients by an associative brain-computer interface. J. Neurophysiol. 115, 1410–1421. https://doi.org/10.1152/jn.00918.2015.

Müller-Putz, G.R., Scherer, R., Brunner, C., Leeb, R., Pfurtscheller, G., 2008. Better than random? a closer look on BCI results. Int. J. Bioelectromagn. 10, 52–55.

Muthukumaraswamy, S.D., 2013. High-frequency brain activity and muscle artifacts in MEG/EEG: a review and recommendations. Front. Hum. Neurosci. 7, 138. https://doi.org/10.3389/fnhum.2013.00138.

Nolan, H., Whelan, R., Reilly, R.B., 2010. FASTER: fully automated statistical thresholding for EEG artifact rejection. J. Neurosci. Methods 192, 152–162. https://doi.org/10.1016/j.jneumeth.2010.07.015.

Nunez, P.L., Srinivasan, R., 2006. Electric Fields of the Brain. Oxford University Press https://doi.org/10.1093/acprof:oso/9780195050387.001.0001.

Ono, T., Shindo, K., Kawashima, K., Ota, N., Ito, M., Ota, T., Mukaino, M., Fujiwara, T., Kimura, A., Liu, M., Ushiba, J., 2014. Brain-computer interface with somatosensory feedback improves functional recovery from severe hemiplegia due to chronic stroke. Front. Neuroeng. 7, 19. https://doi.org/10.3389/fneng.2014.00019.

Park, W., Kwon, G.H., Kim, Y.-H., Lee, J.-H., Kim, L., 2016. EEG response varies with lesion location in patients with chronic stroke. J. Neuroeng. Rehabil. 13, 21. https://doi.org/10.1186/s12984-016-0120-2.

Pereira, J., Ofner, P., Schwarz, A., Sburlea, A.I., Müller-Putz, G.R., 2017. EEG neural correlates of goal-directed movement intention. NeuroImage 149, 129–140. https://doi.org/10.1016/j.neuroimage.2017.01.030.

Pfurtscheller, G., Lopes Da Silva, F.H., 1999. Event-related EEG/MEG synchronization and desynchronization: basic principles. Clin. Neurophysiol. 110, 1842–1857. https://doi.org/10.1016/S1388-2457(99)00141-8.

Pichiorri, F., Morone, G., Petti, M., Toppi, J., Pisotta, I., Molinari, M., Paolucci, S., Inghilleri, M., Astolfi, L., Cincotti, F., Mattia, D., 2015. Brain-computer interface boosts motor imagery practice during stroke recovery. Ann. Neurol. 77, 851–865. https://doi.org/10.1002/ana.24390.

Pineda, J.A., Allison, B.Z., Vankov, A., 2000. The effects of self-movement, observation, and imagination on μ rhythms and readiness potentials (RP's): Toward a brain-computer interface (BCI). IEEE Trans. Rehabil. Eng. 8, 219–222. https://doi.org/10.1109/86.847822.

Pontifex, M.B., Gwizdala, K.L., Parks, A.C., Billinger, M., Brunner, C., 2016. Variability of ICA decomposition may impact EEG signals when used to remove eyeblink artifacts. Psychophysiology 54, 386–398. https://doi.org/10.1111/psyp.12804.

Ramos-Murguialday, A., Birbaumer, N., 2015. Brain oscillatory signatures of motor tasks. J. Neurophysiol. 113, 3663–3682. https://doi.org/10.1152/jn.00467.2013.

Ramos-Murguialday, A., Soares, E., Birbaumer, N., 2010. Upper limb EMG artifact rejection in motor sensitive BCIs. In: 32nd Annual International Conference of the IEEE Engineering in Medicine and Biology Society (EMBC), pp. 1–6. https://doi.org/10.1109/IEMBS.2010.5735240.

Ramos-Murguialday, A., Schürholz, M., Caggiano, V., Wildgruber, M., Caria, A., Hammer, E.M., Halder, S., Birbaumer, N., 2012. Proprioceptive feedback and brain computer interface (BCI) based neuroprostheses. PLoS One 7, e47048. https://doi.org/10.1371/journal.pone.0047048.

Ramos-Murguialday, A., Broetz, D., Rea, M., Läer, L., Yilmaz, O., Brasil, F.L., Liberati, G., Curado, M.R., Garcia-Cossio, E., Vyziotis, A., Cho, W., Agostini, M., Soares, E., Soekadar, S., Caria, A., Cohen, L.G., Birbaumer, N., 2013. Brain-machine interface in chronic stroke rehabilitation: a controlled study. Ann. Neurol. 74, 100–108. https://doi.org/10.1002/ana.23879.

Ray, A.M., López-Larraz, E., Figueiredo, T.C., Birbaumer, N., Ramos-Murguialday, A., 2017. Movement-related brain oscillations vary with lesion location in severely paralyzed chronic stroke patients. In: 39th Annual International Conference of the IEEE Engineering in Medicine and Biology Society (EMBC), pp. 1664–1667. https://doi.org/10.1109/EMBC.2017.8037160.

Rehme, A.K., Eickhoff, S.B., Wang, L.E., Fink, G.R., Grefkes, C., 2011. Dynamic causal modeling of cortical activity from the acute to the chronic stage after stroke. NeuroImage 55, 1147–1158. https://doi.org/10.1016/j.neuroimage.2011.01.014.

Sannelli, C., Vidaurre, C., Müller, K.-R., Blankertz, B., 2016. Ensembles of adaptive spatial filters increase BCI performance: an online evaluation. J. Neural Eng. 13, 046003. https://doi.org/10.1088/1741-2560/13/4/046003.

Savić, A., Lontis, R., Jiang, N., Popović, M., Farina, D., Dremstrup, K., Mrachacz-Kersting, N., 2014. Movement related cortical potentials and sensory motor rhythms during self initiated and cued movements. In: Jensen, W., Andersen, O.K., Akay, M. (Eds.), Replace, Repair, Restore, Relieve-Bridging Clinical and Engineering Solutions in Neurorehabilitation. Biosystems & Biorobotics, Springer International Publishing, pp. 701–707. https://doi.org/10.1007/978-3-319-08072-7.

Schlögl, A., Keinrath, C., Zimmermann, D., Scherer, R., Leeb, R., Pfurtscheller, G., 2007. A fully automated correction method of EOG artifacts in EEG recordings. Clin. Neurophysiol. 118, 98–104. https://doi.org/10.1016/j.clinph.2006.09.003.

Schwarz, A., Ofner, P., Pereira, J., Sburlea, A.I., Müller-Putz, G.R., 2018. Decoding natural reach-and-grasp actions from human EEG. J. Neural Eng. 15, 016005. https://doi.org/10.1088/1741-2552/aa8911.

Seeber, M., Scherer, R., Muller-Putz, G.R., 2016. EEG oscillations are modulated in different behavior-related networks during rhythmic finger movements. J. Neurosci. 36, 11671–11681. https://doi.org/10.1523/JNEUROSCI.1739-16.2016.

Shiman, F., López-Larraz, E., Sarasola-Sanz, A., Irastorza-Landa, N., Spueler, M., Birbaumer, N., Ramos-Murguialday, A., 2017. Classification of different reaching movements from the same limb using EEG. J. Neural Eng. 14, 046018. https://doi.org/10.1088/1741-2552/aa70d2.

Stępień, M., Conradi, J., Waterstraat, G., Hohlefeld, F.U., Curio, G., Nikulin, V.V., 2011. Event-related desynchronization of sensorimotor EEG rhythms in hemiparetic patients with acute stroke. Neurosci. Lett. 488, 17–21. https://doi.org/10.1016/j.neulet.2010.10.072.

Tallon-Baudry, C., Bertrand, O., Delpuech, C., Permier, J., 1997. Oscillatory gamma-band (30-70 Hz) activity induced by a visual search task in humans. J. Neurosci. 17, 722–734. https://doi.org/10.1007/s11064-011-0538-7.

Tangwiriyasakul, C., Mocioiu, V., van Putten, M.J.a M., Rutten, W.L.C., 2014a. Classification of motor imagery performance in acute stroke. J. Neural Eng. 11 https://doi.org/10.1088/1741-2560/11/3/036001. (036001).

Tangwiriyasakul, C., Verhagen, R., Rutten, W.L.C., van Putten, M.J.A.M., 2014b. Temporal evolution of event-related desynchronization in acute stroke: a pilot study. Clin. Neurophysiol. 125, 1112–1120. https://doi.org/10.1016/j.clinph.2013.10.047.

Trincado-Alonso, F., López-Larraz, E., Resquín, F., Ardanza, A., Pérez-Nombela, S., Pons, J.L., Montesano, L., Gil-Agudo, Á., 2018. A pilot study of brain-triggered electrical stimulation with visual feedback in patients with incomplete spinal cord injury. J. Med. Biol. Eng. 38 (5), 790–803. https://doi.org/10.1007/s40846-017-0343-0.

Urigüen, J.A., Garcia-Zapirain, B., 2015. EEG artifact removal—state-of-the-art and guidelines. J. Neural Eng. 12, 031001. https://doi.org/10.1088/1741-2560/12/3/031001.

Velu, P.D., de Sa, V.R., 2013. Single-trial classification of gait and point movement preparation from human EEG. Front. Neurosci. 7, 84. https://doi.org/10.3389/fnins.2013.00084.

Wagner, J., Makeig, S., Gola, M., Neuper, C., Müller-Putz, G., 2016. Distinct beta band oscillatory networks subserving motor and cognitive control during gait adaptation. J. Neurosci. 36, 2212–2226. https://doi.org/10.1523/JNEUROSCI.3543-15.2016.

Walter, A., Ramos-Murguialday, A., Spüler, M., Naros, G., Leão, M.T., Gharabaghi, A., Rosenstiel, W., Birbaumer, N., Bogdan, M., 2012. Coupling BCI and cortical stimulation for brain-state-dependent stimulation: methods for spectral estimation in the presence of stimulation after-effects. Front. Neural Circ. 6, 87. https://doi.org/10.3389/fncir.2012.00087.

Ward, N.S., Brown, M.M., Thompson, A.J., Frackowiak, R.S.J., 2003. Neural correlates of outcome after stroke: a cross-sectional fMRI study. Brain 126, 1430–1448. https://doi.org/10.1093/brain/awg145.

Wright, Z.A., Rymer, W.Z., Slutzky, M.W., 2014. Reducing abnormal muscle coactivation after stroke using a myoelectric-computer interface: a pilot study. Neurorehabil. Neural Repair 28, 443–451. https://doi.org/10.1177/1545968313517751.

Yilmaz, O., Birbaumer, N., Ramos-Murguialday, A., 2015. Movement related slow cortical potentials in severely paralyzed chronic stroke patients. Front. Hum. Neurosci. 8, 1033. https://doi.org/10.3389/fnhum.2014.01033.